PERFORMANCE ANALYSIS OF AN ADVANCED EMISSION REDUCTION TECHNOLOGY ENGINE DURING DIESEL-HYDROGEN DUAL FUEL OPERATION

A Thesis
Submitted to the Graduate Faculty
of the
North Dakota State University
of Agriculture and Applied Science

By

Kirk Jonathan Bottelberghe

In Partial Fulfillment of the Requirements
for the Degree of
MASTER OF SCIENCE

Major Department:
Mechanical Engineering

August 2011

Fargo, North Dakota

North Dakota State University
Graduate School

Title

Performance Analysis of an Advanced Emission Reduction Technology Engine

During Diesel Hydrogen Dual Fuel Operation

By

Kirk Bottelberghe

The Supervisory Committee certifies that this ***disquisition*** complies with North Dakota State University's regulations and meets the accepted standards for the degree of

MASTER OF SCIENCE

ABSTRACT

Bottelberghe, Kirk Jonathan, M.S., Department of Mechanical Engineering, College of Engineering and Architecture, North Dakota State University, August 2011. Performance Analysis of an Advanced Emission Reduction Technology Engine During Diesel-Hydrogen Dual Fuel Operation. Major Professor: Dr. Robert Pieri.

The primary objective of this study was to determine the capability of a CAT engine controlled by an advanced combustion emission reduction technology (ACERT) electronic control module to operate in a dual fuel mode. A CAT 6.6-liter ACERT test engine was outfitted to operate on a hydrogen-diesel fuel mixture. A continuous stream of hydrogen was infused into the intake air charge after the turbocharger. At 50% of rated load, the addition of hydrogen, at three different speeds (1300, 1800, and 2100 RPM), was examined. The hydrogen addition varied from 0-60% of input energy. The maximum amount of hydrogen added before knock occurred, for 1300, 1800, and 2100 RPM, was 54%, 46%, and 55%, respectively. At 1300 RPM, the addition of hydrogen resulted in a decrease in specific energy consumption (SEC) for all levels of hydrogen. For 1800 and 2100 RPM, the SEC improved only when hydrogen was added beyond 46% and 55%, respectively. Emissions testing, while using hydrogen, showed a consistent decrease in carbon dioxide (CO_2) emissions and an increase in nitrogen oxides (NO_x) emissions for all test speeds. The carbon monoxide (CO) emissions showed improvement at levels of hydrogen exceeding 40% for all test speeds. The hydrocarbon (HC) emission did not vary during the addition of hydrogen.

TABLE OF CONTENTS

LIST OF TABLES

LIST OF APPENDIX TABLES

LIST OF FIGURES

LIST OF APPENDIX FIGURES

LIST OF ACRONYMS

ACERT	Advanced Combustion Emission Reduction Technology
BDC	Bottom Dead center
BTDC	Before Top Dead Center
C_3H_8	Propane
CAT	Caterpillar
CH_4	Methane
CI	Compression Ignition
CO	Carbon Monoxide
CO_2	Carbon Dioxide
DOC	Diesel Oxidation Catalyst
DPF	Diesel Particulate Filter
ECM	Electronic Control Module
EGR	Exhaust Gas Recirculation
EGT	Exhaust Gas Temperature
EOI	End Of Injection
EPA	Environmental Protection Agency
EU	European Union
H_2	Hydrogen
H_2O	Water
HC	Hydrocarbon
IC	Internal Combustion

IVC	Intake Valve Close
MFB	Mass Fraction Burn
N_2	Nitrogen
NDSU	North Dakota State University
NMHC	Nonmethane Hydrocarbon
NO	Nitrogen Oxide
NO_2	Nitrogen Dioxide
NO_x	Nitrogen Oxides
O_2	Oxygen
O_3	Ozone
Pb	Lead
PM	Particulate Matter
PPM	Parts Per Million
r_c	Compression Ratio
RPM	Revolution Per Minute
SCR	Selective Catalytic Reduction
SEC	Specific Energy Consumption
SI	Spark Ignition
SOI	Start Of Injection
TDC	Top Dead Center
US	United States
VGT	Variable Geometry Turbine

VR	Variable Reluctance
VVT	Variable Valve Timing

CHAPTER 1. BACKGROUND

Analyzing the world use of petroleum and the resulting pollution will examine the relevance of reducing petroleum consumption. The broad field of alternative fuels proposed as a solution will be narrowed down to address one avenue of potential use in the overview of internal combustion (IC) engines. Relevant information about IC engine operation will be provided throughout the overview of IC engines and the combustion chemistry and resulting emissions sections. Lastly, current efforts addressing the problem will be explained in the emission control strategies section.

1.1. World Use of Petroleum

There has been a large amount of research focused on the amount of petroleum available because of its widespread use throughout the world. Petroleum is used in numerous products such as plastics, detergents, agricultural products, asphalt, lubricants, and primarily transportation fuels [1]. The use of petroleum has increased for roughly the past 8 decades [1]. The increased demand in the last three decades has largely been due to the transportation sector [2]. The transportation sector is comprised of vehicles traveling by road, rail, air, and water [3]. Petroleum is the main supply of energy for the transportation sector. In 2009, it accounted for 94% of the energy supply to that sector [1]. The transportation sector is projected to grow through 2035, and the consumption of petroleum is projected to increase, as well. A 45% increase in liquid-fuels consumption from 2007-2035 in the transportation sector is projected [3]. Liquid

fuels are composed of conventional petroleum and unconventional fuels such as biofuels, coal-to-liquids, oil sands. Petroleum accounted for approximately 94% of the liquid fuels in 2007 [3]. The transportation sector is identified as the main driver for the growth of oil demand [2].

The increasing use of petroleum has raised concerns about when the supply of oil will be exhausted. Before the world supply of oil is exhausted, an event called peak oil will occur, which is when the maximum production of oil is reached, and in subsequent years, not as much is produced because of limited availability. Predictions of when peak oil will occur are varied. Some predictions state peak oil will occur between the years 2015-2035 [4]. The outcome of peak oil will create a "severe liquid fuels problem for the transportation sector" [5]. The decline in oil production is expected to have a dramatic increase in petroleum prices [5, 6]. The reliance of the transportation sector on petroleum, and the concern about its continual availability, has increased interest in, and the relevance of, alternative energy research.

An effect of the growing transportation sector, besides an increase in petroleum consumption, is an increase in vehicle emissions. The common means of powering vehicles in the transportation sector is an IC engine which has emissions from combustion of petroleum products. The road portion of the transportation sector includes cars, light duty trucks, freight trucks, sport utility vehicles, motorcycles, buses, etc. The rail portion consists of trains used for transportation of goods or people, which includes light-rail, commuter, and freight

trains. The water section includes recreational craft, tugboats, barges, and freighters. All of these mentioned vehicles typically use an IC engine and have emissions.

The United States (US) Environmental Protection Agency (EPA) has termed emissions which could be harmful to people as criteria pollutants. The criteria pollutants are carbon monoxide (CO), lead (Pb), ozone (O_3), nitrogen dioxide (NO_2), particulate matter (PM), and sulfur dioxide (SO_2) [7]. CO, NO_2, and PM are emitted from combustion of petroleum typically used in motor vehicles. The CO emissions from the transportation sector account for approximately 90% of the US's CO emissions. Similarly, the transportation sector accounts for 55% of the US's nitrogen oxides (NO_x) emissions and 6% of the PM emissions [8]. The transportation sector is a major contributor to air pollution, and motor vehicle emissions are the largest contributor to smog [9]. Smog is a pollutant which forms when sunlight interacts with NO_x [10]. The concern about air pollution from vehicle emissions makes alternative fuels a significant field of research because of the potential for pollutant reduction. Alternative energy sources are being investigated and used by the transportation sector to meet today's energy demand.

More specifically, there is a focus on alternative energy used in IC engine operation. One alternative fuel for the future is hydrogen because it has "potential as a long-term alternative to petroleum-based liquid fuels" [5]. Using hydrogen as a fuel source displaces the input of petroleum fuel used during combustion and is one way to decrease IC engine emissions. The combustion of hydrogen and

resulting emissions will be examined in more detail throughout the background section.

To successfully reduce consumption of petroleum and pollution production, alternative fuels have to be produced through renewable/sustainable paths. Hydrogen is an alternative fuel which has the potential of being produced sustainably. Using electricity from petroleum to convert water into hydrogen still relies on petroleum to produce hydrogen, and the pollutants from burning petroleum are still emitted. Sustainable methods which are cost-competitive (based upon optimistic technology improvements) for producing hydrogen are wind, biological, and thin-film solar processes [11]. Another potential approach is hydrogen derived directly from biomass. The ability to produce hydrogen via renewable paths, and the potential to decrease harmful emissions, has led to considering it as an alternative fuel source for IC engines and fuel cells. The remainder of this paper focuses on the use of hydrogen in IC engines, as opposed to fuel cells, because of the widespread use of IC engines.

1.2. Overview of Internal Combustion Engines

Internal combustion engines have several common distinguishing features and a distinct purpose. IC engines are used to convert chemical energy (gasoline for example) into mechanical work. This is achieved by combusting an energy source in a closed chamber. That distinguishing process is indicative of the name internal combustion. The combustion is used to force a piston down a cylinder and do work. A common practice is to omit the prefix 'reciprocating' from IC engines

although not all IC engines are reciprocating [12]. A reciprocating motion means the piston only travels down the cylinder so far before returning back up. Figure 1 helps show the reciprocating process [13]. After the combustion in step 1, the piston travels down the cylinder and rotates the shaft to which it is attached. When it reaches the bottom, the rotational energy in the shaft starts to move the piston back up the cylinder as shown in step 2. This is a reciprocating process and is another distinguishing feature of IC engines. The majority of IC engines use a reciprocating process because it results in useful rotational energy.

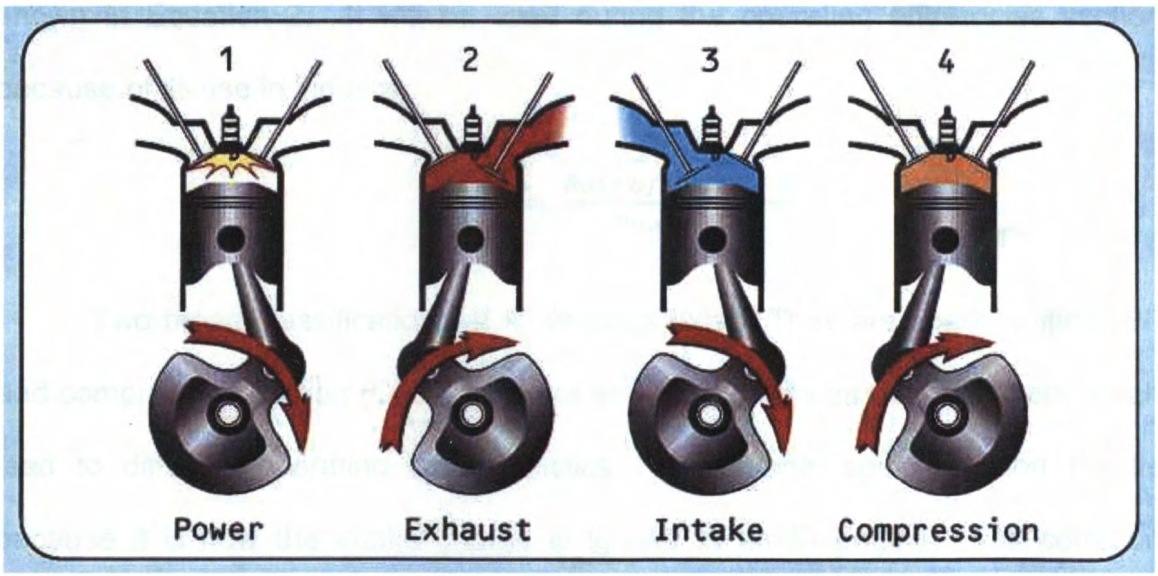

Figure 1: Four-stroke operating cycle in an IC engine [13].

When energy conversion takes place, an efficiency is commonly associated with that process in order to evaluate the completeness of the conversion. One common efficiency used to evaluate the performance of IC engines is the brake thermal efficiency. The brake thermal efficiency is the work out divided by the

amount of energy in [13]. This is shown in Equation 1. The term brake means the work output is an experimentally measured value.

$$\eta_b = \frac{Work_{out}}{Energy_{in}} \tag{1}$$

Another way of examining the efficiency is the specific energy consumption (SEC), the rate of energy consumption per unit power. The SEC is more commonly used in industry because engineers are more concerned with the amount of energy required to produce a specific power output [12]. The SEC is shown in Equation 2. It will be used during the operating efficiencies section because of its use in industry.

$$SEC = \frac{Rate\ of\ Energy\ in}{Power\ out} \tag{2}$$

Two broad classifications of IC engines exist. They are spark ignition (SI) and compression ignition (CI). There are several differences between them which lead to different operating characteristics. The name 'spark' ignition results because it is how the intake charge is ignited in an SI engine. The common practice of producing a spark is to use a spark plug. The intake charge is composed of a homogenous air-fuel mixture which is compressed. The amount of compression is termed the compression ratio. The compression ratio is the ratio of the maximum volume to the minimum volume. The maximum volume occurs when the piston is at bottom dead center (BDC) and the minimum volume occurs when the piston is at top dead center (TDC). The compression ratio (r_c) is shown in Equation 3.

$$r_c = \frac{Volume_{TDC}}{Volume_{BDC}} \quad (3)$$

SI engines typically have a compression ratio ranging from 8:1-12:1 [16]. In an SI engine, a throttle blade is used to control the amount of air-fuel mixture sucked into the intake. Controlling the amount of air-fuel mixture in the intake available for combustion controls the power output. The induction of the air-fuel mixture from the intake into the combustion chamber is controlled by the intake valves' opening and closing, valve timing. The valve timing is a set engine parameter which is not directly varied by the operator. The use of a throttle blade introduces pumping losses in an SI engine. The pumping losses result in lower work output.

The thermodynamic model of an SI engine is the Otto Cycle. A pressure vs. specific volume diagram of an ideal, four stroke, Otto Cycle is shown in Figure 2. The four strokes in a four stroke engine are: 1) compression stroke; 2) power stroke; 3) exhaust stroke; 4) intake stroke. The compression stroke occurs from 1-2 in Figure 2. A constant volume heat addition occurs from 2-3 and is the thermodynamic representation of constant volume combustion. Constant volume combustion is a distinguishing trait of an SI engine. The power stroke occurs from 3-4. This is followed by a constant volume heat release from 4-5, which is termed blowdown. The exhaust stroke occurs from 5-6, and the intake stroke is from 6-1.

The second broad classification of an IC engine is a CI engine. In a CI engine, the start of combustion occurs when the fuel-air mixture self-ignites. The

fuel-air mixture is compressed until an appropriate temperature and pressure are reached and then combustion starts. The self-ignition pressure and temperature are fuel dependent [12]. Typical compression ratios range from 12:1-24:1 [16]. The higher compression ratio compared to an SI engine is used to reach the self-ignition point of the fuel. The power output is controlled by controlling the amount of fuel added to the combustion chamber. This requires no throttle blade because the fuel is injected directly into the chamber. There are lower pumping losses than what occur with an SI engine.

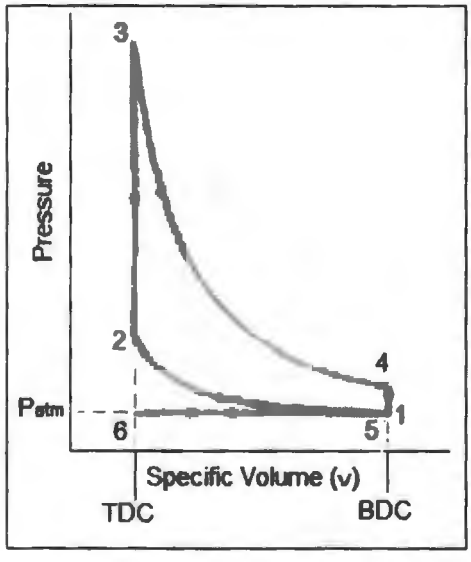

Figure 2: Ideal Otto Cycle.

The thermodynamic model for a CI engine is the Diesel Cycle. A pressure vs. specific volume diagram for an ideal, four stroke, Diesel Cycle is shown in Figure 3. The compression stroke occurs from 1-2 in Figure 3. A constant pressure heat addition occurs from 2-3 and is the thermodynamic representation of constant pressure combustion. Constant pressure combustion is a characteristic

of a CI engine. The power stroke occurs from 3-4. This is followed by a constant volume heat release from 4-5, exhaust blowdown. The exhaust stroke occurs from 5-6 and the intake stroke is from 6-1.

The intake charge in a CI engine is composed solely of air. The fuel is injected directly into the combustion chamber just before combustion, and this does not allow adequate time for the fuel to be evenly dispersed amongst the intake charge. This results in a heterogeneous mixture inside the combustion chamber prior to, and during, combustion. The typical CI combustion process has several distinct phases: atomization, vaporization, mixing, self-ignition, and combustion [16]. Atomization, vaporization and mixing make up the ignition delay period during combustion [12].

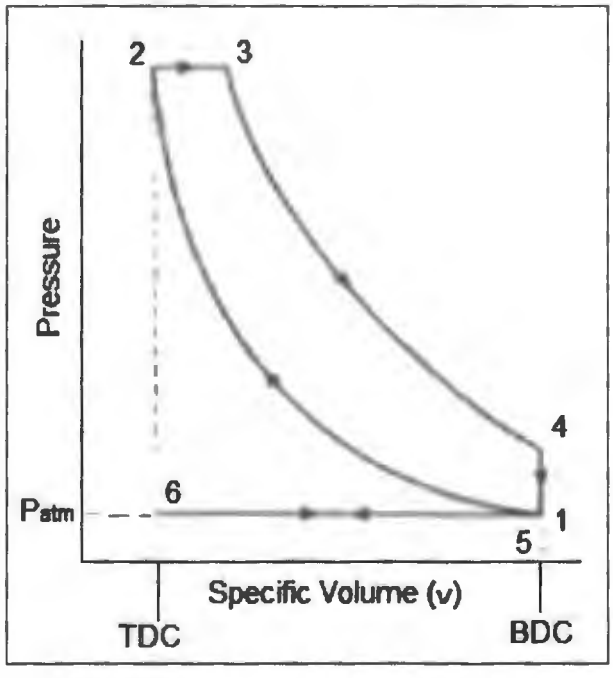

Figure 3: Ideal Diesel Cycle.

The first step during ignition delay is atomization. Atomization is where the fuel is injected with a high velocity to increase the mixing with air and to disperse the fuel throughout the cylinder. The high velocity is achieved by using high fuel pressure. During the injection, the fuel forms very small droplets. Higher injection pressure aids in creating smaller droplets and greater droplet dispersal. The very small droplets then evaporate. This happens very readily due to the high temperature from compressing the air [16]. Smaller droplet size results in a more rapid evaporation. As the fuel drops evaporate, the surrounding temperature decreases. This aids in incomplete evaporation of the fuel. Due to a combination of high droplet concentration and cooling from evaporation, localized saturation occurs [16]. The fuel vapor must mix with air in the combustion chamber to form a mixture which has an appropriate air to fuel ratio for combustion. The fluid motion of the intake charge and high injection velocity enhance mixing within the combustion chamber. Mixing is important for preventing saturated areas of fuel and incomplete use of oxygen during combustion.

Once the fuel is prepared, hot spots are the initial ignition sites. Self-ignition occurs, simultaneously, at numerous sites throughout the combustion chamber. The ignition reactions are exothermic and increase the local temperature. The increase in temperature leads to more self-ignition, and it eventually leads to a sustained combustion, which is the final step. Numerous flame fronts spread across the combustion chamber consuming all the fuel with an appropriate air to fuel ratio. Poor fuel dispersion in the combustion chamber results in unused fuel and poor fuel economy. A very quick rise in pressure and temperature is

associated with this step [16]. Figure 4 shows the progression of diesel combustion with respect to crank angle [17]. At a timing of -7°, the fuel streams are visible, and fuel preparation is occurring. Between -7° and -3°, self-ignition occurs. The counterclockwise curve shape of the flame illustrates the swirl motion of the intake charge within the combustion chamber. Sustained combustion is occurring from TC (Top Center) to 30°.

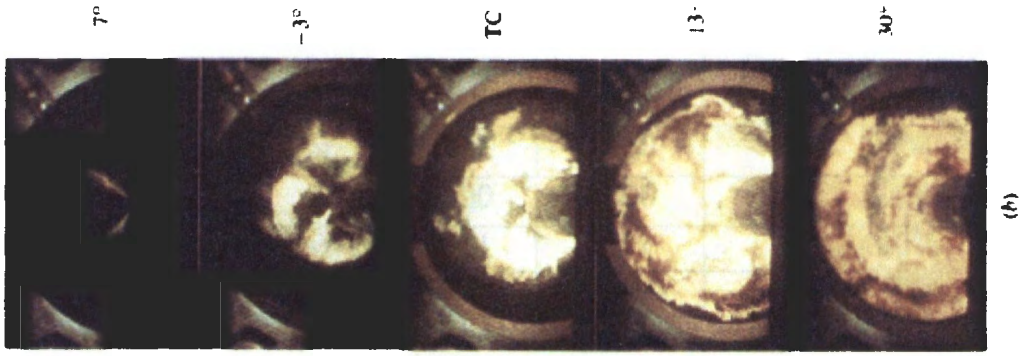

Figure 4: Progression of diesel combustion [17].

Some relevant values during CI combustion are the flame temperature, flame speed, and self-ignition temperature. A comparison between the values from stoichiometric hydrogen and diesel combustion provides background information for the analysis of dual fuel combustion, or rather when two different fuels are consumed during combustion. The use of dual fuel combustion through the remainder of this paper refers to the use of hydrogen and diesel as the two fuel sources. The values from hydrogen and diesel combustion are presented in Table 1.

Diesel fuel has a self-ignition temperature of around 630°F, a flame temperature of roughly 3500°F, a laminar burning velocity of 1.64 ft/s, and a lower heating value of 19300 BTU/lbm [12, 18]. Comparatively, during stoichiometric hydrogen combustion, the self-ignition temperature is 1080°F, the flame temperature is 3800°F, the laminar burning velocity is 9.51 ft/s, and the lower heating value is 61000 BTU/lbm [18].

Table 1: Typical combustion values for diesel and hydrogen.

	Diesel	Hydrogen	Percent Increase from diesel to hydrogen
Auto Ignition Temperature (°F)	630	1080	71%
Flame Temperature (°F)	3500	3800	8.6%
Laminar Burning Velocity (ft/s)	1.64	9.51	480%
Lower Heating Value (BTU/lbm)	19300	61000	220%

The auto ignition temperature of hydrogen is 71% higher than diesel and is the reason diesel is used as a pilot fuel to ignite hydrogen in dual fuel operation. The flame temperatures of diesel and hydrogen are the most similar, with hydrogen being 8.6% higher. The laminar flame speed of diesel and hydrogen vary greatly. During stoichiometric combustion, hydrogen has a laminar flame speed 480% greater than diesel.

A laminar flame speed is not totally representative of what occurs during combustion. Combustion in a CI engine is very turbulent and a laminar burn does not occur. Diesel combustion is diffusion controlled combustion. Diffusion controlled means the fuel (diesel) and air enter the combustion zone separately and are required to mix prior to burning [12, 19]. Figure 5 shows the difference

between a laminar flame front and a turbulent flame front in diffusion controlled combustion [12]. The turbulence (labeled order of air motion in Figure 5) aids in sweeping the fuel vapor away from the fuel droplet and allowing air to mix with the fuel. The turbulence during diesel combustion increases the speed of combustion by an order of magnitude by aiding in the mixing process [12].

The combustion of hydrogen during dual fuel experimentation at NDSU is both pre-mixed and non-stationary combustion. This means the fuel (hydrogen) and air are mixed prior to combustion and the flame front travels through the air-fuel mixture [19]. Turbulence aids in increasing the speed of combustion by increasing the flame front area [12].

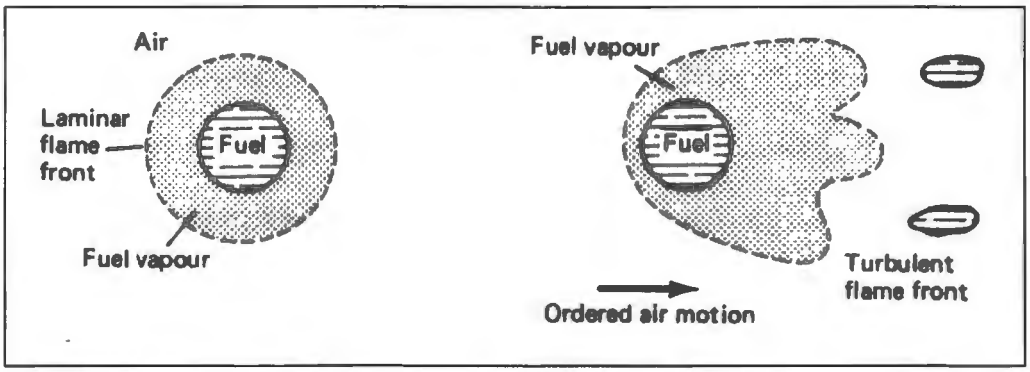

Figure 5: Difference between laminar and turbulent flame front during diffusion controlled combustion [12].

Figure 6 shows a comparison between laminar and turbulent flame fronts during pre-mixed combustion. The turbulent speed of hydrogen combustion is higher than its laminar combustion speed, but it is of the same order of magnitude [20]. Further discussion about factors, such as turbulence and pressure, influencing flame speed during hydrogen combustion is provided by Verhelst [18].

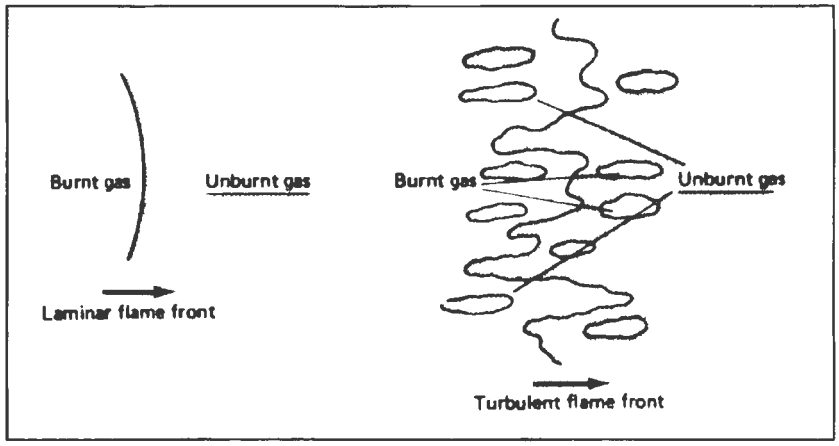

Figure 6: Comparison between laminar and turbulent flame fronts during pre-mixed combustion [12].

In order to combust the fuel in the chamber, oxygen needs to be present. Oxygen is introduced by using atmospheric air for combustion, which is composed of roughly 79% nitrogen and 21% oxygen by volume [13]. The limited time and flow losses during induction and the large presence of nitrogen make it a challenge to provide oxygen for combustion. A typical way of increasing the amount of oxygen is to use a turbocharger.

A turbocharger consist of several sections working together to convert the exhaust gas energy to useful work. The main systems of a turbocharger are the turbine wheel, center section, and compressor wheel which are shown in Figure 7 [15]. The exhaust gases are used to spin the turbine wheel. The center section contains the bearings which support the shaft connecting the turbine wheel and compressor wheel. As the turbine wheel spins, the compressor wheel rotates also. The compressor wheel draws in ambient air and compresses it. The amount of compression and resulting pressure rise is termed boost. By increasing the

pressure of the compressed air flow, more oxygen can be introduced for combustion.

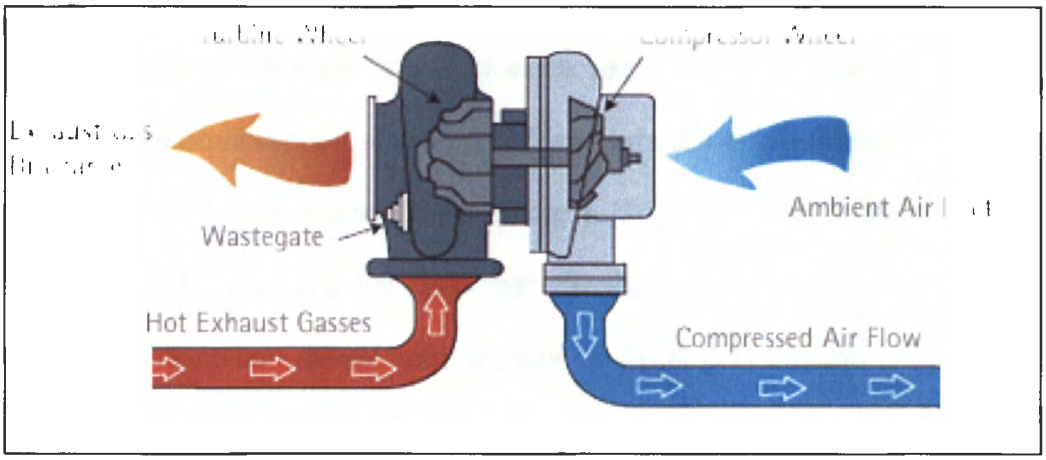

Figure 7: Turbocharger sections [15].

An operating limit experienced by CI engines is knock. Engine knock is spontaneous uncontrolled combustion, which has detrimental effects to the engine [12]. During engine knock, there is a characteristic 'rapid' pressure rise, pressure spikes occurring throughout combustion, and a characteristic knocking noise [12, 21]. Knock in a CI engine occurs from self-ignition occurring too slowly [12]. When self-ignition occurs too slowly, too much fuel is injected into the chamber before combustion starts, and this results in an excess fuel mixture ready for combustion. Once self-ignition occurs, the properly mixed fuel combusts rapidly and results in a 'rapid' pressure rise. The fuel injection rate is a designed engine parameter set to avoid excessive injection of fuel before self-ignition, which avoids knock. During knock, the engine structure experiences vibrations. Cracks can result from this leading to component failure. Methods of detecting knock are examining pressure curves from combustion and audible detection [22].

Compression ignition engines are widely used throughout the world in numerous applications. They play a large role in transportation vehicles, nonroad equipment, and stationary power generation sites. Currently in the US, 650,000 pieces of nonroad equipment are sold each year, and there are approximately 6 million pieces of equipment in use [23]. Diesel cars (CI engines) are widely used in Europe and account for roughly 50% of sales [24, 25]. Based off the number of vehicles sold in Europe in 2006, and the assumption that 50% are diesels, there were roughly 7.9 million diesel vehicles sold in 2006 [24, 25, 26]. The ability to operate CI engines on alternative fuels, namely hydrogen, allows for a large positive global impact to result, pending successful incorporation.

1.3. Combustion Chemistry and Resulting Emissions

The fuel input for combustion in a CI engine is typically a hydrocarbon fuel. An example of a hydrocarbon fuel is propane (C_3H_8). The input fuel needs oxygen (O_2) which is supplied by air for combustion. In an ideal reaction, the reactants are converted into water vapor (H_2O), carbon dioxide (CO_2), and nitrogen gas (N_2). A stoichiometric combustion reaction is shown in Equation 4.

$$C_3H_8 + 5(O_2 + 3.76N_2) \rightarrow 4H_2O + 3CO_2 + 18.8N_2 \quad (4)$$

This reaction has the appropriate amount of oxygen so there is the complete combustion of fuel to CO_2 with no extra oxygen. Complete combustion means all input carbon reacted to form CO_2 with no extra oxygen. The nitrogen part of air is usually considered stable unless high temperatures are present. The reaction presented is composed of reactants, substances which undergo combustion, and

products, the results of combustion [14]. The combustion reaction is balanced. This means there is an equal number of each element in the reactants and products. For example, there are 3 carbon atoms in the reactants and 3 carbon atoms in the products.

The combustion reaction presented is an ideal reaction and does not account for the formation of pollutants such as CO, PM, hydrocarbons (HC), or NO_x. NO_x is the sum of nitric oxide (NO) and NO_2. NO_x formation is "strongly dependent on temperature, local concentration of oxygen, and the duration of combustion" [12]. High combustion temperatures are the primary factor [12, 16]. The formation of CO occurs from areas which are 'rich'. Rich refers to the air to fuel ratio and means there is more fuel than air for ideal stoichiometric combustion. Another way of describing when rich occurs is when there is not enough air for stoichiometric combustion. The lack of oxygen prevents complete formation of CO_2 [16]. HC and PM formation results from incomplete combustion of the fuel [12, 16].

The problem of pollutants being introduced into the atmosphere from combustion has raised environmental concerns. Countries throughout the world have implemented regulations to control the output of pollutants. In the US, government standards set by the EPA were imposed to decrease nonroad CI engine emissions. Nonroad equipment includes recreational vehicles, farm and construction equipment, boats, and locomotives [23]. The EPA gradually reduced the legal level of emissions over the years for various sizes of engines used in

nonroad equipment. The changes are known as tiers. Starting at Tier 1, in 1996, the EPA has progressed to the current Interim Tier 4 which became effective in 2011. The EPA predicts an annual reduction of 738,000 tons of NO_x emissions when the old fleet of nonroad equipment has met Final Tier 4 regulations [23]. Figure 8 shows the decrease in emissions regulated by the EPA for an engine with a power rating between 175 and 299 horsepower.

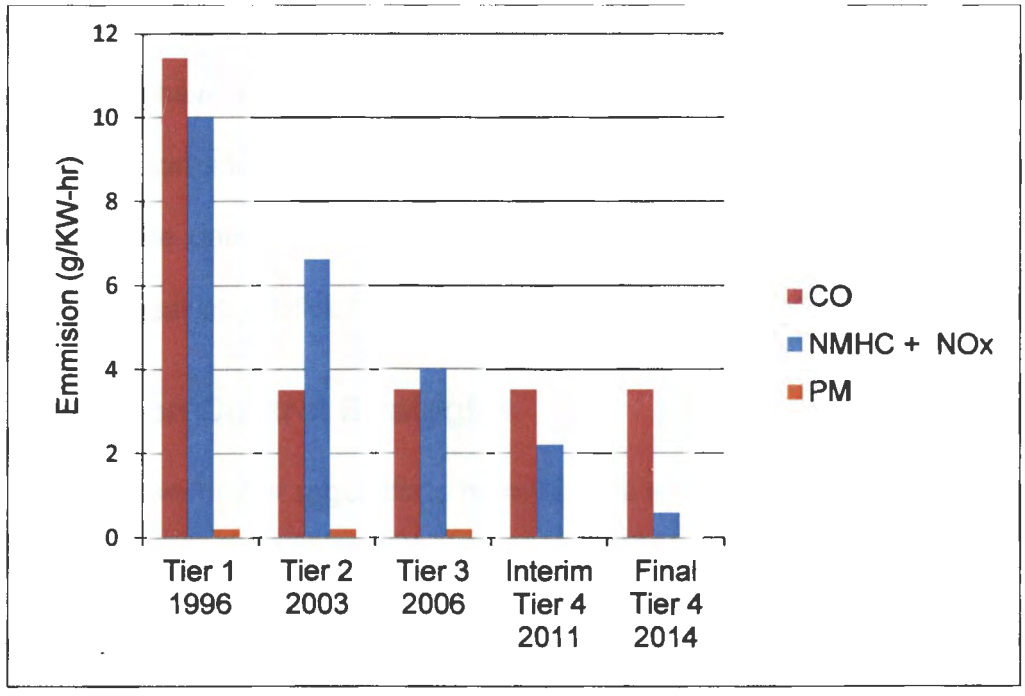

Figure 8: EPA regulated nonroad diesel emissions decrease for a 175-299 horsepower engine.

NMHC stands for non-methane hydrocarbon. This includes all hydrocarbons expect methane, and is regulated by the EPA. Methane (CH_4) is a hydrocarbon that is not included in the EPA's regulations on decreasing HC emissions because it does not harmfully react with the atmosphere [16]. The transition from Interim Tier 4 to Final Tier 4 is the last reduction. It requires a 73%

reduction in NMHC + NO_x emissions, and PM and CO emissions must remain the same as Interim Tier 4. PM emissions for Tier 4 are very minimal in Figure 8. From Tier 3 to Interim Tier 4, PM was reduced by 90% from 0.2 to 0.02 g/KW-hr. It must remain at 0.02 g/KW-hr.

In Europe, similar standards are being implemented by the European Union (EU). The EU's Stage III B and Stage IV are similar to Interim Tier 4 and Final Tier 4, respectively. Both the European and US regulations monitor the same emissions and have similar limits. For example, EU Stage IV and EPA Final Tier 4 both have the same limit for NMHC + NO_x [27]. The largest difference between the standards is the date the regulations are enforced. The EU Stage IV becomes effective one year after EPA Final Tier 4.

1.4. Emission Control Strategies

With government regulations mandating a reduction in emissions, a variety of emission control solutions have been developed. These solutions address the global problem of air pollution from using petroleum in IC engines. A brief background about each control strategy will be discussed. The six strategies covered are: 1) exhaust gas recirculation (EGR); 2) a variable geometry turbine (VGT) combined with EGR; 3) exhaust after-treatments; 4) variable valve timing (VVT); 5) common rail fuel injection strategies; 6) alternative fuels.

Exhaust Gas Recirculation: A common strategy for reducing emissions is EGR. As the name implies, exhaust gas is re-circulated from the exhaust stream into the intake air stream. The re-circulated portion of the exhaust gas is typically

cooled prior to entering the intake air stream. By introducing exhaust gas back into the combustion chamber via the intake air stream, the cylinder temperatures during combustion are reduced [12, 27, 28]. The reduction of temperature results in less NO_x formation. A downside of using EGR is loss in power. With intake air being replaced by exhaust gas, the oxygen available for combustion decreases resulting in a loss of power [33].

Variable Geometry Turbine with EGR: A VGT changes the pitch of the turbine blades to control the rotational speed of the compressor wheel. This allows the turbocharger to control the level of boost over a wider range of engine speeds. Using a VGT enables higher rates of EGR to be used without losses in power. The ability of the VGT to maintain a required boost level through a wide range of engine speeds enables a larger mass of intake charge to be forced into the combustion chamber. The VGT is able to counteract the decrease of air (oxygen) in the intake charge from EGR by increasing boost [27, 30]. This allows for further use of EGR which further reduces NO_x emissions.

Exhaust After-treatment: After-treatment options include diesel oxidation catalyst (DOC), diesel particulate filter (DPF), and selective catalytic reduction (SCR). DOC relies upon chemical reactions to reduce emissions. The exhaust gas travels through the DOC which oxidizes the gaseous HCs and PM. DOCs typically reduce carbon monoxide by 40%, hydrocarbons by 50%, and PM by 20% [27]. A DPF does exactly as the name implies; it filters the PM from the exhaust. The exhaust gas travels through a filter which traps and holds the PM, thereby

reducing PM emission [27]. SCR is a method of reducing NO_x emissions by relying on chemical reactions. SCR sprays urea, an ammonia and water mixture, into the exhaust gas. The exhaust gas passes through a catalytic converter which starts a chemical reaction. The byproducts of the chemical reaction are nitrogen, oxygen, and water [27]. Use of SCR has reduced NO_x emissions up to 90% [31].

Variable Valve Timing: Variable valve timing controls the opening, closing, amount of lift, and phasing of the intake and exhaust valves on an engine. Basically, VVT allows extensive control of the combustion charge, or rather, the gases trapped in the combustion chamber before combustion. VVT reduces emissions by reducing the cylinder pressure and temperatures [32]. By controlling when the intake valve closes (IVC), the effective compression rate can be decreased, and lower cylinder pressure and temperatures are achieved. With late IVC, the maximum volume of the cylinder and chamber is reduced before compression starts. The effective compression ratio is the ratio of the volume at IVC to the volume at TDC. The emission of NO_x is decreased because of the reduced temperature [32].

Common Rail Fuel Injection Strategies: The use of a common rail system makes advanced fuel injection methods capable and has reduced emissions [33]. By using the fuel pump to pressurize the common rail, which stores the fuel, the fuel will always be pressurized. Older systems used the fuel pump for injection purposes, which eliminated the possibility for multiple injections and made the injection pressure dependent upon engine speed. New common rail systems are

capable of multiple injections and high injection pressure throughout the engines operating range. Multiple injections and higher injection pressures result in a more complete combustion [27]. The improved combustion reduces the level of HC, PM and CO emissions.

Alternative Fuels: The driving source for the emissions reduction when using alternative fuels is the change in the chemical composition of the input fuel. As mentioned in the brief overview of combustion chemistry, the amount of elements used as reactants equals the amount of elements leaving as products. Changing the chemical composition of the fuel, only, isn't enough to reduce emissions. Efficient combustion must still occur. One alternative fuel which reduces emissions is biodiesel. The chemical composition of biodiesel contains oxygen. The presence of oxygen in the fuel aids in combustion, and reductions in CO, HC, and PM result from biodiesel combustion [34]. Another alternative fuel is hydrogen. When used with diesel in dual fuel operation, hydrogen provides energy which displaces the input of petroleum-based fuel. Improvements in combustion and the reduction of carbon in the fuel result in reductions of NO_x, HC, PM, and CO emissions during dual fuel operation [35, 36, 37].

Of the emission control strategies covered, using hydrogen and biodiesel are the two solutions which address both the reduction of petroleum and emissions. The remainder of this research will focus on using hydrogen in CI engines to reduce the consumption of petroleum-based fuels and to lower emissions.

The use of hydrogen in a CI engine, as opposed to an SI engine, is being analyzed because CI engines are used extensively in nonroad applications across the world. Nonroad engines are faced with upcoming emission regulations and hydrogen has potential to help meet those regulations. Compression ignition engines are more efficient than SI engines. They have a higher thermal efficiency than SI engines because they operate at higher compression ratios [12]. They have less pumping losses because they operate without a throttling device in the air stream. They also have a 98% burn efficiency which is better than SI engines [12]. The higher efficiency and widespread use in nonroad equipment were the determining factors to pursue hydrogen use in CI engines.

CHAPTER 2. LITERATURE REVIEW

The literature review will focus on the operation of a CI engine in dual fuel mode and how it aids in reducing petroleum consumption and decreasing harmful emissions. The various approaches of hydrogen injection in CI engines will be examined in the hydrogen addition strategies and hydrogen addition coupled with emission control strategies sections. The results and limitations of dual fuel operation will be examined in the engine performance changes section. The North Dakota State University (NDSU) Engine Research Lab and ACERT ECM control strategies sections provide information which helped determine the specific research objective and challenges within it.

2.1. Hydrogen Addition Strategies

The approach to introduce hydrogen into the combustion chamber has varied in recent research. The three different ways of introducing hydrogen into the combustion chamber are direct injection, injection into the intake manifold, and a continuous infusion into the intake air charge [35, 38, 39]. Figure 9 shows the varying locations used to inject hydrogen [15].

The direct injection approach introduces hydrogen directly into the combustion chamber. In Figure 9, it is labeled as 1. Direct injection offers the most control of hydrogen injection. The timing, quantity, and rate of hydrogen injection can be readily controlled by an electronic control module (ECM). Direct injection is the safest injection method because it eliminates the potential for backfires. The injection timing and duration are independent of valve timing. After

the intake valve is closed, hydrogen can be introduced into the combustion chamber eliminating the possibility of a backfire. The drawback to this system is the cost of incorporating a high pressure injector into the cylinder head and an ECM to an existing engine.

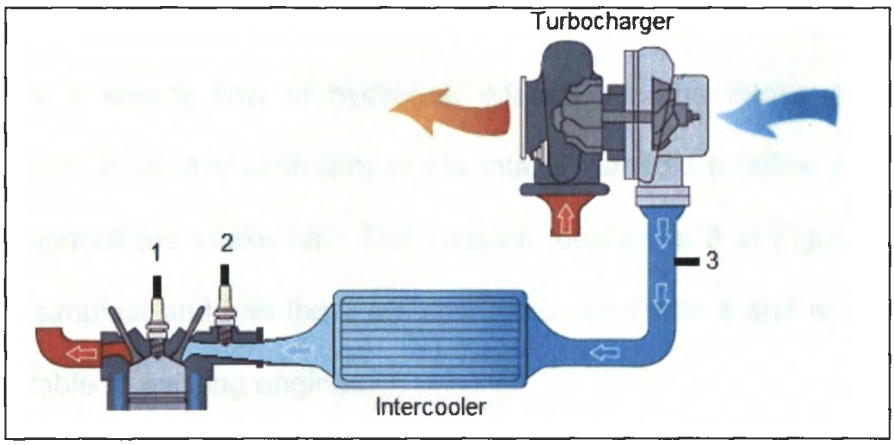

Figure 9: Varying locations used to inject hydrogen [15].

The second approach is intake manifold injection. It uses an electronically controlled injector to injection hydrogen into the intake air charge. The injector is located in the intake runner close to the intake valve. The location of injection is labeled as 2 in Figure 9. Intake manifold injection requires the added cost of an electronic injector, but the injector is not exposed to the same high pressures as the direct injection method. This setup does not offer as much control over hydrogen injection as compared to the direct injection method. The injection timing of hydrogen is constrained by the intake valve timing. This method relies on the hydrogen entering the combustion chamber with the intake air charge. When the intake valve is closed, no more hydrogen can be introduced into the combustion chamber. Since the hydrogen enters the combustion chamber with the intake air

charge, there is time for hydrogen to mix with the air prior to combustion. The possibility of backfires is greater in intake manifold injection than in direct injection. Flow reversal during the intake stroke could result in hydrogen in the intake runner which could backfire if ignited.

The third approach to introducing hydrogen is continuous hydrogen infusion. This setup has a steady flow of hydrogen infused into the intake air charge. Hydrogen infusion is usually upstream of the intake manifold to allow diffusion of hydrogen throughout the intake air. The infusion location is 3 in Figure 9. This method is the simplest and has the least cost associated with it and is, therefore, the most adaptable to existing engines.

The drawbacks of continuous infusion are the potential for uneven hydrogen distribution to all cylinders in a multi-cylinder engine, as well as backfires. The distribution of hydrogen is dependent upon the design of the intake manifold. Intake manifolds are designed to evenly disperse the intake air to all cylinders so uneven hydrogen dispersion is not a large concern. Backfires are a potential concern because a flammable hydrogen-air mixture travels through the intake ducting. A hot spot within the ducting may ignite the mixture.

Continuous infusion is the approach used to introduce hydrogen at NDSU Engine Research facilities. Studies using intake manifold injection and continuous infusion methods are relevant to research conducted at NDSU because both injection methods have a similar hydrogen air mixture entering the combustion chamber.

2.2. Hydrogen Addition Coupled with Emission Control Strategies

The testing platforms used during dual fuel testing have varied throughout recent research. The difference among the testing platforms results from the possibility of employing different emission control strategies with the addition of hydrogen. Several experiments use testing platforms which do not employ any emission control strategies presented besides hydrogen addition [35, 37, 38, 40, 41, 42]. They are operating with a single, fixed, mechanical fuel injection. A couple testing platform use one emissions control strategy along with the addition of hydrogen, such as EGR [36], or common rail fuel injection [43]. Other testing platforms incorporate multiple emission control strategies with the addition of hydrogen. Hydrogen is added to engines which use common rail fuel injection, turbochargers, and EGR [44, 46].

2.3. Engine Performance Changes

This section will review the results from the addition of hydrogen in several common areas that are covered in current research of dual fuel CI engine operation. These common areas are engine operating efficiency, exhaust emissions, and operating limit imposed by knock.

A method of analyzing engine operating efficiency is to evaluate the brake thermal efficiency. Brake thermal efficiencies have been noted to increase with the addition of hydrogen [35, 36, 41, 42]. The increase in thermal efficiency was attributed to a more complete combustion process [35, 36]. The faster burn rate of a hydrogen-air mixture was responsible for a more complete combustion. The

increase in efficiency was noted in research with testing platforms which did not use a common rail fuel injection system. In research which used a common rail system, no clear trend between hydrogen addition and brake thermal efficiency was evident [43]. The use of a common rail system allows for a more complete combustion process and reduces the improvements in combustion from the addition of hydrogen.

The addition of hydrogen has resulted in a decrease of several exhaust gases. The exhaust gases analyzed in research are CO, CO_2, HC, PM and NO_x. Of these exhaust gases analyzed, CO_2 is not a regulated emission by US standards. It is included in current research because of global warming concerns [45]. The topic of global warming is outside the research of this study, but CO_2 emissions will be included because of the information they offer to other research.

Carbon dioxide reduction occurred in engines with and without EGR when hydrogen was added. When hydrogen was implemented into the combustion process, CO_2 emission decreased [35, 36, 37]. Its reduction is linked to the reduction in carbon input for combustion. The engine operating without EGR exhibited a larger reduction in CO_2 compared to engines operating with EGR. The use of EGR introduces already formed CO_2 back into the intake charge. The addition of already formed CO_2 to combustion results in more CO_2 in the exhaust. Engines operating without EGR had a larger reduction in CO_2 because no CO_2 was introduced into combustion.

The results of CO and HC emissions were similar to the CO_2 emissions during the addition of hydrogen. As hydrogen was added, CO and HC emissions decreased because of less carbon input in combustion [35, 36, 37]. Engine operation without EGR exhibited larger CO and HC reduction as compared to engine operation with EGR. EGR has different effects on CO and HC formation than it does on CO_2 formation. The use of EGR reduces the amount of input oxygen. This, in turn, reduces the strength of combustion which lowers combustion temperatures. With lower combustion temperatures and less oxygen, the oxidation reaction to form CO_2 is weakened and incomplete combustion creates CO and HC. This accounts for an increase in CO and HC emissions [36].

The addition of hydrogen resulted in a decrease in NO_x emissions in several studies [35, 37, 43, 46], but it also showed an increase in others [36, 46]. NO_x formation is "strongly dependent on temperature, local concentration of oxygen, and the duration of combustion" [12]. The decrease in NO_x emissions was believed to occur from two different scenarios which were a decrease in exhaust gas temperature (EGT) and lean burn combustion [35, 37]. Lower EGTs decreased NO_x emissions because temperatures were not sufficient to initiate NO_x formation. The importance of a lean burn operation is the lack of oxygen for the formation of NO_x even though a lean burn is typically associated with higher exhaust temperatures [16]. With the total consumption of oxygen, none was present for NO_x formation.

A decrease in NO_x emission as hydrogen was added resulted while the injection timing was allowed to drift (retard) [46]. The importance of mentioning the timing drift is to point out that two variables changed with the addition of hydrogen. A second experiment was conducted which isolated the timing change. It retarded the injection without adding hydrogen. The second experiment exhibited a decrease in NO_x similar to hydrogen addition, but a noticeable increase in SEC [46]. These results led to further experiments which added hydrogen and held the injection timing constant. The experiments with set injection timing and the addition of hydrogen exhibited a slight increase in NO_x formation. The sequence of experiments illustrated that hydrogen addition with set injection results in increased NO_x formation. When coupled with retarding injection timing, NO_x emissions were reduced while SEC was maintained [46].

An increase in NO_x emission resulted as hydrogen was added [36]. The increase in NO_x was linked with an increase in EGT. Higher exhaust temperatures resulted in an increase in secondary reactions during combustion leading to higher NO_x formation.

As described previously, a limiting factor for CI engine operation is knock. It was examined during current dual fuel research. Two main methods of analyzing knock were used in the research, 1) examination of pressure curves from combustion combined with audible detection and 2) the rate of mass fraction burned (MFB). Analysis of pressure curves and audible detection are accepted methods for knock detection but fail to provide a quantitative comparison [22]. By

using pressure curves from combustion and audible detection, knock was determined to occur when 30% of the input energy for combustion was hydrogen [38].

Several papers failed to mentioned their method analyzing knock except that it was occurring [35, 37]. To classify the level of knock beyond occurrence was not necessary because its presence eliminated that operating condition. No comparison about the quantity of hydrogen, which caused engine knock, was capable because the percent of input energy from hydrogen was not provided.

Another research group recommended the maximum amount of hydrogen added to the combustion process was 15% energy [40]. This recommendation was based on engine durability. An in-depth analysis of engine knock was conducted to justify that recommendation. The method used to analyze knock was the rate of mass fraction burn (MFB). The MFB rate is used to classify the burn rate of fuel during combustion. A peak MFB rate higher than conventional diesel would signify a higher engine knock than that for which the engine was designed. The input fuel burns more rapidly and produces a more pronounced force on the combustion chamber and piston face. At hydrogen levels of 15% energy and less, the rate of MFB was less than conventional diesel. The engine, therefore, experienced combustion which did not exceed the design limit. Without exceeding the design constraints, engine durability would not be compromised.

2.4. NDSU Engine Research Lab

North Dakota State University Engine Research lab has studied dual fuel operation in CI engines since 2005. There has been a consistent progression of research in analyzing the capabilities of hydrogen use in CI engines. Initial research studied the possibility of operating a CI engine in dual fuel mode and determined it was possible. Further research explored the limits of engine operation in dual fuel mode [38]. These initial experiments were conducted with a mechanically controlled engine which had a fixed, single fuel injection.

The growing use of electronics and implementation of new emission control strategies resulted in the engine used for experimentation to become outdated. North Dakota State University Engine Research labs continued to grow in the field of dual fuel operation by updating the test facilities. A new engine used for research at NDSU operates with a current electronic control system. It utilizes a common rail fuel system to carry out advanced fuel injection strategies to control combustion and the resulting emissions.

2.5. ACERT ECM Control Strategies

The new engine acquired for experimentation at NDSU is a Caterpillar (CAT) 6-cylinder, 6.6-liter engine. It is controlled by an ACERT ECM. ACERT is a CAT trademark which was incorporated to meet upcoming emission standards imposed by the federal government [10]. The test engine uses a high pressure common rail fuel delivery system with injection pressures up to 2000 bar. The

control algorithms used to monitor and control the engine are proprietary information.

Some of the different operating regimes in ACERT technology are multiple injections per power stroke. Varied injection pulses are incorporated to offer precise control of fuel input. Figure 10 shows a voltage signal sent to the injector for 1350 RPM and 300 ft-lbs of torque. The injection method used consists of a pilot injection followed by the primary injection. The primary injection consists of short microbursts after the 0.25 ms main voltage pulse. The ACERT ECM uses precise electronic control to improve combustion [47].

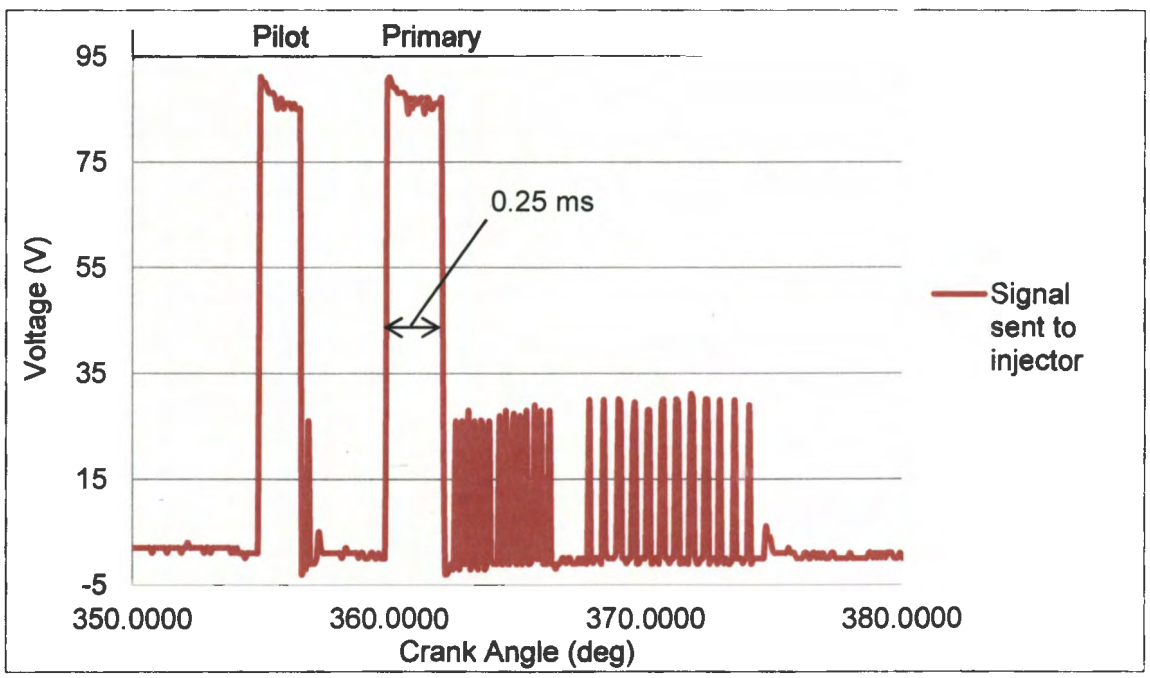

Figure 10: Voltage signal sent to injector at 1350 RPM and 300 ft-lbs of torque.

Another variable which was adjusted to control combustion was the injection timing. The separation between the pilot and primary injection changed, as well as

the timing of when the injection started. In Figure 10, the pilot injection occurs at roughly 355 degrees, 5 degrees before top dead center (BTDC), but as the engine speed increases, the pilot injection occurs sooner. At 2100 RPM and 175 ft-lbs, the pilot injection occurs at roughly 350 degrees, 10 degrees BTDC, and the primary injection occurs at 359 degrees, 1 degree BTDC. The injection timing was varied to control the timing of peak pressures relative to TDC. Currently no research has implemented hydrogen infusion with a CAT ACERT ECM.

CHAPTER 3. RESEARCH OBJECTIVE

The first and primary objective of this research is to determine the capability of a CAT 6-cylinder, 6.6-liter ACERT engine to operate with a continuous flow hydrogen infusion system. The timing of the pilot injection raises a concern about ignition starting too early and about detrimental effects occurring to the engine. The ability of the ACERT ECM to adapt to hydrogen addition, and to maintain engine performance, is questionable and will be monitored. A second objective is to determine the percent of input energy (diesel) which can be replaced by hydrogen before knock limits engine operation. The use of a common rail injection system and the advanced injection methods of ACERT change the combustion and the amount of hydrogen addition before knock is unknown. The third objective is to quantify changes in emissions and engine efficiencies as hydrogen is added.

CHAPTER 4. RESEARCH IMPORTANCE

The objectives of this research aid in reducing consumption of petroleum-based fuel and reducing harmful emissions from CI engines. Continuing hydrogen substitution research in CI engines provides important knowledge and advancements about applications which offer potential to have a large impact because of the widespread use of CI engines. Studying the effects that the addition of hydrogen has during combustion in a CAT ACERT engine is applicable across multiple engines using similar high pressure common rail fuel systems. Aside from reducing petroleum consumption, using hydrogen aids in reducing emissions. The reduction of harmful emissions, such as CO, HC, and NO_x, results from the addition of hydrogen. Not only is this important for the environment, but it also brings nonroad engines closer to meeting Final Tier 4 emission regulations.

CHAPTER 5. RESEARCH APPROACH

The approach used during this research consisted of two main systems. The first system was the experimental setup which was the equipment used during data collection and the engine modifications required to outfit the test setup with sensors. The second system was the experimental procedure which was the process followed during data collection.

5.1. Experimental Setup

The experimental setup consisted of four subsystems: 1) the engine and ECM subsystem; 2) the hydrogen infusion subsystem; 3) the data acquisition subsystem; 4) the exhaust gas analysis subsystem.

Engine and ECM Subsystem: Several engine modifications were conducted to outfit the engine with sensors. Pressure transducers were inserted into cylinders 3 and 6. The pressure transducers replaced the glow plugs. The concern of removing glow plugs from some cylinders, and affecting engine performance, was irrelevant because glow plugs are used during cold startups which did not occur during testing. The placement of the pressure transducer was constrained by the presence of intake valves, exhaust valves, and the fuel injector. The placement of the pressure transducer within the combustion chamber is shown in Figure 11.

The decision to place the pressure transducer in the glow plug hole provided for the best placement, as well as for the easiest insertion. The glow plug hole placed the pressure transducer closest to the center of the combustion

chamber without jeopardizing the cylinder head structure. Placing the pressure transducer close to the center of the combustion chamber eliminated unwanted pressure spikes from pressure waves reflecting off the cylinder wall. The pressure transducers used were AutoPSI-S 0-3000 psi sensors produced by Optrand Inc. in Michigan. They were optical sensors which consisted of a deformable membrane that reflected light. The light was transmitted down a fiber optic cable to the calibrated processor. The processor output was a voltage ranging from 0.5-5 volts. The sensors were calibrated by the company and the specific sensitivities were stamped on them.

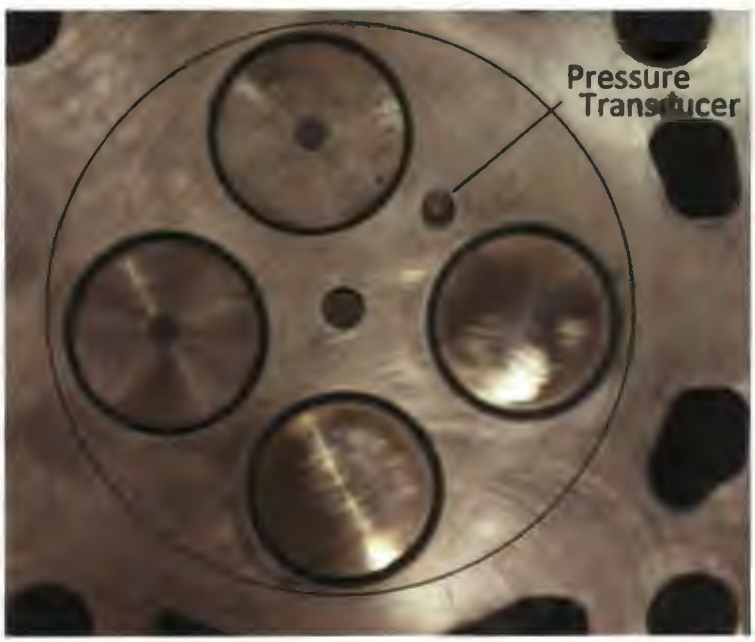

Figure 11: Pressure transducer placement within cylinder head.

A variable reluctance (VR) position indicator was fitted to the flywheel. It was timed to indicate when cylinder 6 was at TDC. The procedure for finding TDC for cylinder 6 consisted of installing a dial indicator in the injector hole and a timing

wheel on the front of the engine. The engine was rotated until piston 6 was roughly at TDC. The dial indicator and timing wheel were zeroed. The engine was rotated clockwise until the piston moved 0.1 inches down the cylinder bore. The degree marking on the timing wheel was noted. The engine was then rotated counterclockwise until the piston was 0.1 inches down the cylinder bore. The degree marking on the timing wheel was noted. The average between the two timing marks was found and the engine was turned to it. The degree wheel was then adjusted to read TDC and the dial indicator was zeroed. The process was repeated to verify that the average value of the degree markings resulted, again, in TDC. This process was conducted to obtain an accurate reference for TDC because there is minimal piston movement compared to crank rotation when the engine is at TDC (piston dwell). The proper installation of the VR sensor and pick up were verified by comparing the timing of the TDC signal to a pressure curve. The indication for TDC occurred 0.8 degrees after peak pressure in a pressure curve from cranking the engine. This exhibited the expected behavior for a properly timed indicator [21]. For a direct-injection CI engine, the peak pressure should occur in a range of 0.8-1 degree BTDC [21].

The engine setup had a coolant system which was regulated by electronic controllers. The coolant system had two loops. The first loop was for engine coolant and had a water to water heat exchanger. The second loop was for the intake air charge that had an air to water heat exchanger. The electrical system consisted of a JLD-612 Temperature Controller for each loop which pulsed the coolant water through the heat exchanger to maintain the loop at the set

temperature. The pulsing of water sent pressure waves through the water lines which in turn affected the water pressure delivered to the water break dynamometer. During certain operating conditions, the load exerted by the dynamometer fluctuated slightly with the varying water pressure. This fluctuation was accounted for by conducting longer tests at set points and averaging the data.

Hydrogen Infusion Subsystem: This subsystem consisted of four main components: 1) the hydrogen storage tank; 2) the pressure regulator; 3) the hydrogen mass flow meter; 4) the variable flow control valve. These components are numbered in Figure 12 [38].

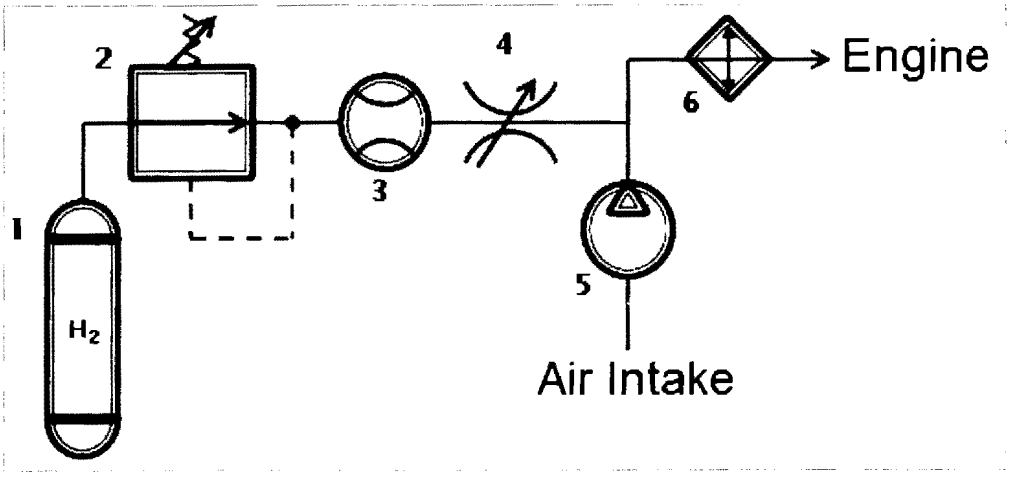

Figure 12: Hydrogen infusion schematic [38].

The hydrogen storage bottle is number 1. It stored hydrogen at 2000 psi. The pressure regulator is number 2. It reduced the pressure from the tank to 80 psi to protect the downstream mass flow meter. The mass flow meter is number 3. It was a model 10A Gas Flow Meter produced by Fox Thermal Instruments in California, and it was specifically calibrated for hydrogen flow. Two probes were

introduced into the flow, and one probe was held at a constant temperature while the other changed temperature to match the flowing hydrogen. The power required to produce the heat flux necessary to maintain the constant temperature probe was calibrated to a mass flow rate. The needle valve is number 4 and was used to control the flow rate of hydrogen into the intake air stream. The turbocharger and intercooler are numbers 5 and 6, respectively. The hydrogen was infused into the air intake stream after the turbocharger and before the intercooler. The location for hydrogen infusion was selected for sufficient diffusion and safety. Hydrogen infusion after the turbocharger avoided high turbocharger temperatures which could have potentially caused a backfire. The infusion of hydrogen prior to the intercooler forced the hydrogen to pass through the turbulent intercooler which aided in producing a homogenous hydrogen-air mixture.

Data Acquisition Subsystems: There were three different data acquisition systems used throughout the experiments. The first was the DYNOmite-Pro produced by Land and Sea in New Hampshire. It collected engine operating data at a low frequency (2 Hz). Numerous K-Type thermocouples produced by Tempco monitored engine operating temperatures such as intake air, coolant, and exhaust temperatures. A Floscan model 236C flow meter manufactured in Seattle was used to monitor fuel flow. A Land and Sea 13 inch water brake dynamometer was used to load down the engine. The water brake dynamometer had a rotating rotor and fixed stator. The rotor sheared the water against the stator. The force exerted against the stator was reacted to a brace which had a strain gauge. The deformation of the strain gauge was output as a voltage signal. The strain gauge

was calibrated by attaching a lever to the brace and applying a known load to the lever. The calibration torque was then set in the software. The dynamometer had a magnetic pickup which was used to calculate engine speed. The dynamometer attached directly to the crankshaft so the speed registered by the dynamometer was the engine speed. A weather station was used to collect air conditions in the cell. The weather station measured ambient air temperature, humidity, and air pressure. A sample of the data collected from the DYNOmite-Pro acquisition system is included in Appendix A in Table 2.

The second data acquisition system was a DI-710 produced by DATAQ Instruments. This system was used to record the output signal from an Optrand pressure sensor (i.e. cylinder pressure). This system was run at a frequency of 14.4 kHz to capture in cylinder combustion. Since combustion occurs very rapidly, the high frequency was necessary. The DATAQ DI-710 had a maximum total sampling rate of 14.4 kHz. Using only one channel allowed sampling at 14.4 kHz. If two channels were used, the maximum sampling rate per channel would be 7.2 kHz because the maximum total sampling rate was 14.4 kHz. Since using more channels reduced the sampling rate per channel, another data acquisition system was used to record combustion and injection timing. A sample of the data collected from the DATAQ acquisition system is included in Appendix A in Table 3.

The third data acquisition system was a model GDS-2204 digital storage oscilloscope produced by GW Instek in New Taipei City, Taiwan. This system recorded data at 10 kHz which was its maximum. The VR signal, cylinder pressure

signal, and the voltage signal sent to the fuel injector were recorded. This system recorded data used to determine the timing of combustion and injection events. A sample of the data collected from the GW Instek oscilloscope is included in Appendix A in Table 4.

Exhaust Gas Analyzer Subsystem: A Model 7466 Engine Exhaust Analyzer produced by Nova Analytical Systems in New York was used to monitor the exhaust gas. It was a vacuum type analyzer which sampled exhaust from the gas stream and monitored the CO_2, CO, O_2, HC, NO and NO_2. The O_2, CO_2, and CO were presented as a percent; whereas, the HC, NO, and NO_2 were presented in parts per million (PPM). The test meter had a resolution of 1 PPM for HC, NO, and NO_2 and read down to zero. For CO_2 and O_2, the exhaust analyzer had a resolution of 0.1% and read down to zero. For CO, the exhaust gas analyzer had a resolution of 0.01% and read down to zero. The exhaust gas analyzer was serviced and recalibrated by Nova Analytical Systems within the last year, and it was used for experimentation before a recalibration was recommended by the company. The exhaust was sampled 12 inches after the exit of the turbocharger. A bung was welded onto the exhaust, and a sampling tube was inserted through it into the middle of the exhaust stream. An air tight seal was achieved to ensure only exhaust gas was sampled, and air in the test cell was not polluted. A sample of the data collected from the Nova Exhaust Gas Analyzer is included in Appendix A in Table 5.

5.2. Experimental Procedure

The procedures followed during data collection consisted of a startup procedure which brought the engine up to operating temperature. After startup, several different procedures were followed depending on which data was collected. Figure 13 shows the flow of procedures. There was a procedure for collecting injection timing, operating conditions during dual fuel mode, and a shutdown procedure. The purpose of following these procedures was to ensure consistent and comparable results.

Startup Procedure: The startup procedure consisted of initially inspecting the fluid levels of the engine and visually inspecting the engine to ensure that it was clear of debris, or tools. The electronic power sources, such as exhaust gas analyzer, hydrogen flow meter, pressure transducers, and data acquisition systems, were started and allowed to warm up for 30 minutes. After the electrical warm up period, the electronics were zeroed. The warm up period and zeroing was done to eliminate electrical drift. Next, the engine was started and run for approximately 15 minutes before experiments were conducted. The run time was dictated by the coolant and exhaust temperatures. After the engine coolant and exhaust temperatures reached a steady operating condition, the engine was considered to be warmed up.

Setting RPM and Load Procedure: After the engine went through the startup procedure, data was collected under steady state conditions. The engine was brought to the appropriate load and RPM and allowed to stabilize. The

stabilization time was typically around one minute. The data was collected for a 30 second time interval. The oscilloscope was used to record the voltage signal sent to the fuel injector and TDC timing mark. Data collection using the oscilloscope was a 50 ms run recording at a frequency of 10 kHz.

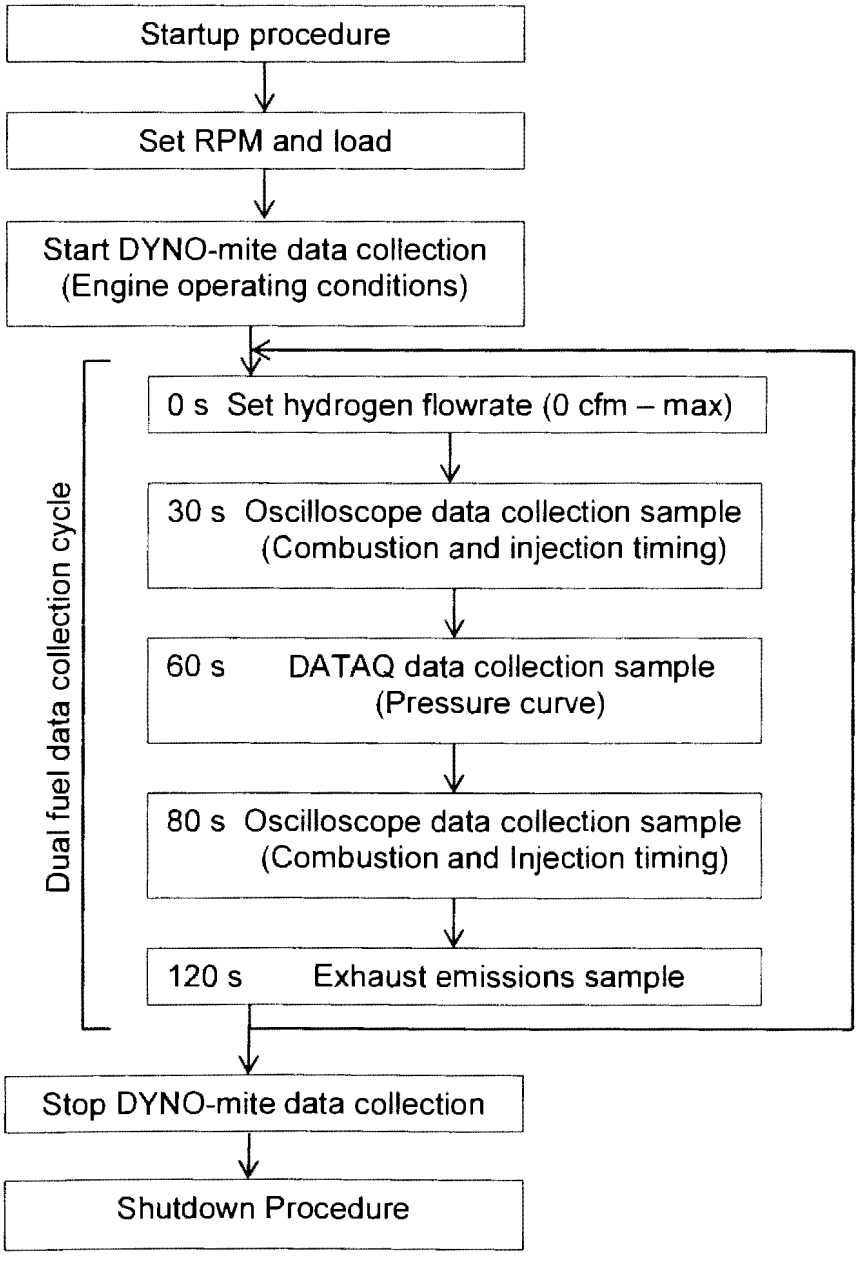

Figure 13: Dual fuel testing procedure.

Starting DYNO-mite Data Collection Procedure: After the startup procedure was conducted, the engine was brought to a specific speed and load. All testing was conducted, at a specific speed, at 50% load. Once the speed and load were set, the DYNO-mite data acquisition system was started and was run for the duration of the test. Next, the dual fuel data collection cycle was started. The first step was to set the hydrogen flow rate. This was increased from 0 cubic feet per minute to the knock operating limit. Next, an oscilloscope sample was collected. Oscilloscope samples collected data about combustion and injection timing. Then, a DATAQ pressure transducer signal, followed by another oscilloscope sample, was collected. Finally, an exhaust emissions reading was collected before the dual fuel data collection cycle started again. Collecting data with different data acquisition systems was done because of the different sampling rate capabilities of each system. (These capabilities were discussed in the experimental setup section of this paper.)

Dual Fuel Data Collection Cycle: After setting the hydrogen flow rate (0 s), the engine was allowed to adjust for 30 seconds. The first combustion and injection timing data collection (oscilloscope data) was done roughly 30 seconds into the cycle. The DATAQ pressure transducer signal was recorded around 60s into the cycle. The second combustion and injection timing data collection was recorded at 80 s. Finally, the exhaust emissions were recorded at 120 s. That completed one dual fuel data collection cycle. The hydrogen flow level was increased, and another cycle was started. This data collection order was followed to allow time for the emissions to stabilize. Preliminary exhaust testing indicated

that NO_x emission levels did not stabilize until about 60 s after a hydrogen change. NO_x emissions rapidly changed as the hydrogen level was changed. Following the rapid change, the NO_x continued to slowly change until about 60 s; therefore, exhaust emissions were recorded about 120 s.

Shutdown procedure: The shutdown procedure had the engine run at idle for roughly 5 minutes. This was done to allow the turbocharger temperature to decrease. Instant shutdown after hard testing could have resulted in oil being left in the turbocharger. It would not have drained completely and the oil could have boiled because of the excessive heat in the turbocharger and this would have ruined the bearings. This procedure was conducted to ensure engine longevity.

The set points which were tested were 1300, 1800, and 2100 RPM. All tests were conducted at 50% of the rated load. These test speeds were chosen because past research at NDSU Engine Research Lab conducted test at these speeds. By continuing testing at these speeds, a larger collection of data could be compiled. Similarly, the amount of hydrogen addition in past NDSU research had been presented and analyzed in percent of input energy. The addition of hydrogen continues, therefore, to be presented in terms of percent of input energy.

CHAPTER 6. RESULTS AND DISCUSSION

The three main topics discussed here are the 1) operating efficiencies, 2) combustion, and 3) emissions. The operating efficiencies section focuses on the substitution of diesel with hydrogen and the resulting changes in SEC. The combustion section analyzes pressure curves, injection changes implemented by the ECM, and the maximum amount of hydrogen substitution before knock limited engine operation. Lastly, the emissions section covers the changes in emissions resulting from hydrogen addition.

6.1. Operating Efficiencies

The addition of hydrogen resulted in a decrease in diesel consumption. Since the engine was held at a fixed load, the amount of input energy required was constant. As hydrogen was infused, the amount of diesel necessary was decreased. Figure 14 shows the relationship between the hydrogen addition and diesel reduction.

Figure 14 contains the test data for hydrogen addition at all three operating speeds. The collected test data is included in Appendix A in Table 1. The energy densities were used to convert the diesel and hydrogen flow rates into energy consumptions. At 1300 RPM, the incremental increase of hydrogen resulted in a linear decrease in diesel fuel input. This is noticeable when analyzing the dark blue curves in Figure 14. The total energy required at 50% load for 1300 RPM remained constant throughout the addition of hydrogen. This was an indicator that

the ECM adapted smoothly to dual fuel operation and decreased the delivery of diesel accordingly.

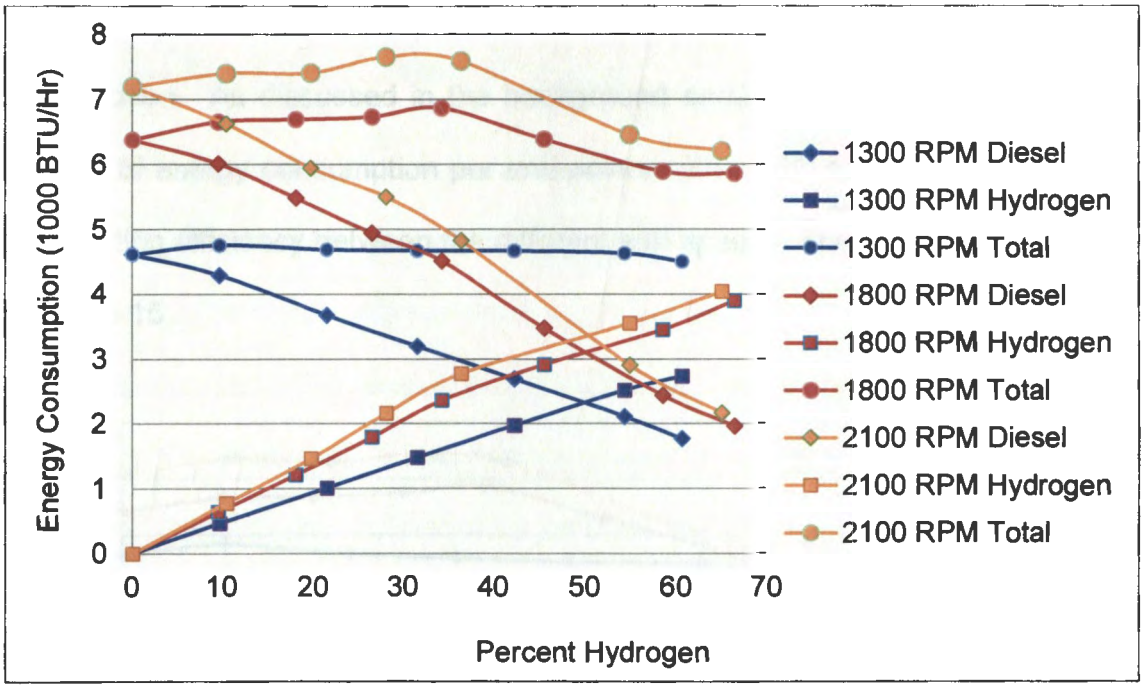

Figure 14: Relationship between hydrogen addition and diesel reduction.

The 1800 and 2100 RPM tests both exhibited a similar linear decrease in diesel as hydrogen was added. The reduction of diesel was not as linear for the 1800 and 2100 RPM test conditions as 1300 RPM. The total energy consumption for both 1800 and 2100 RPM experienced an increase in total energy around 30-40% hydrogen. The analysis of the pressure curves for 1800 and 2100 displayed a shift in pressure curves around those percentages. The shift in the pressure curves are analyzed and discussed in the combustion section. Overall, the total energy used during the 1800 and 2100 RPM test decreased after 40% hydrogen substitution. As a higher percentage of hydrogen was used, the combustion

process improved. The faster combustion of hydrogen resulted in a more complete combustion of the input fuel.

Analysis of the SEC provided a standardized way of analyzing energy consumption. As discussed in the background section of this paper, the SEC is the rate of energy consumption per unit power. The SEC allowed for comparison of operating efficiency between the different test speeds. The SEC data are shown in Figure 15.

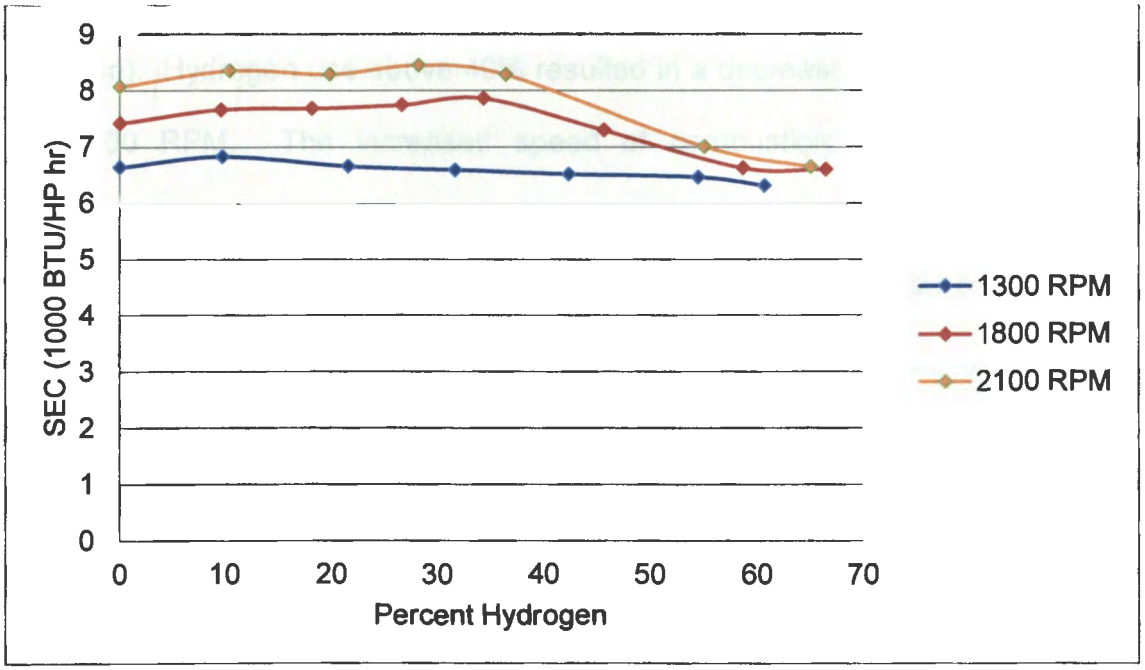

Figure 15: SEC for various test speeds and percentages of hydrogen.

The SEC for 1300 RPM was the lowest throughout all of the tests. The baseline power curve produced peak torque at 1400 RPM. Peak torque was dictated by the camshaft profile and valve timing. With the engine designed to operate most efficiently at 1400 RPM, the 1300 RPM results were expected to

have a low SEC. The 1300 RPM test experienced a slight decrease in SEC as hydrogen was added. During the 1300 RPM test, slight improvements in combustion helped increase the power produced. These improvements are discussed in the combustion section.

The 1800 and 2100 test speeds both experienced a slight increase in SEC around the 30-40% hydrogen addition. The analysis of the pressure curves and discussion in the combustion section explains the increase in SEC. The SEC increased 6% for 1800 and 5% for 2100 relative to the baseline SEC (0% hydrogen). Hydrogen use above 40% resulted in a decrease in SEC for both 1800 and 2100 RPM. The increased speed of combustion, from faster burning hydrogen, resulted in rapid pressure rise occurring just after TDC. This shift in the pressure curve is examined in the combustion section and its connection to improving the SEC is discussed there in more detail. At 55% hydrogen infusion, the SEC at the different test speeds was the closest. Included in Appendix B, is the thermal efficiency for hydrogen addition at the different test speeds. The thermal efficiency is another way of analyzing the same data as the SEC. It is included to provide reference to other engines' thermal efficiencies.

6.2. Combustion

The analysis of combustion was done by using the pressure curves. Both an average waveform and single waveforms were analyzed to determine the combustion characteristics. In order to obtain a characteristic cylinder pressure curve for a testing condition, 15 consecutive pressure curves were averaged to

eliminate slight fluctuations from cycle to cycle. By averaging the pressure curves, knock was filtered out and presented as a smooth pressure profile. This was acceptable for determining pressure variations with hydrogen addition, but was unacceptable for analyzing the operating limit from knock. The single waveforms were solely used for determining the occurrence of knock. They illustrated the pressure spikes occurring during combustion which were characteristic of knock.

The pressure curves for 1300 RPM are presented in Figure 16. The pressure curves indicate that the addition of hydrogen increased the peak pressure, and it occurred earlier during the power stroke. The ECM adapted smoothly to the addition of hydrogen until the highest concentrations. The shape of the pressure curves gradually changed and all maintained the basic profile of the baseline pressure curve. As the basic profile changed, it shifted towards the profile of an SI engine. This gradual shift was responsible for the decrease in SEC. An SI operates on the Otto Cycle which is more efficient than the Diesel Cycle (CI engine) from a thermodynamic standpoint [12,14,and 16]. In actual application, the CI engine is more efficient because it operates at a higher compression ratio and does not encounter throttling. With the addition of hydrogen, the diesel engine started displaying properties of an Otto cycle which made it more efficient, while maintaining the positive characteristics of a diesel. This resulted in a decrease in SEC.

The lowest pressure curve in Figure 16 is the baseline curve. As hydrogen was added, the pressure curves gradually increased. The same basic profile was

maintained during dual fuel operation. Lower amounts of hydrogen, 0-30%, did not result in a rapid pressure rise. The pressure rise remained approximately the same.

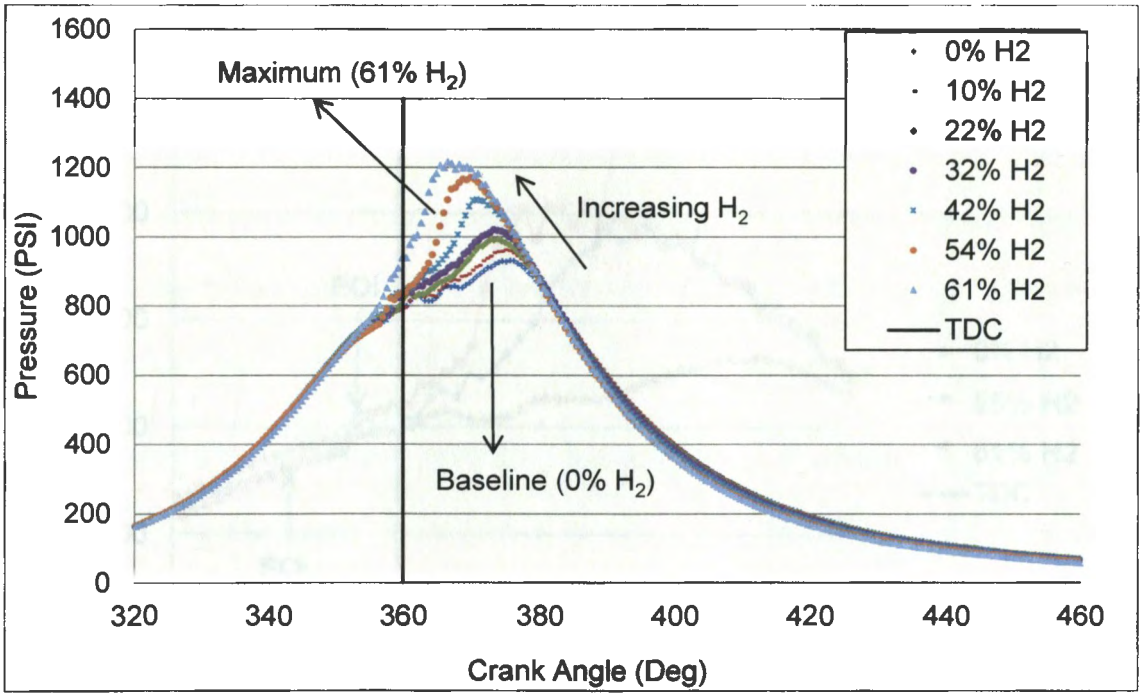

Figure 16: Pressure curves for 1300 RPM with varying percentages of hydrogen.

When 42% hydrogen was added, a different situation occurred. The rate of pressure rise was higher than the previous curves. As hydrogen addition increased past 42%, the rate of pressure rise continued to increase. At 61%, knock started to occur. The noise was the first indication of knock. The pressure curves for the 54% and 61% hydrogen levels were examined to verify that knock was occurring and determine when it began. Figure 17 shows the pressure curves in more detail and includes the baseline pressure curve (0% hydrogen), for reference.

The pressure curve for 60% hydrogen, in Figure 17, illustrates what knock looks like. The rapid increase in pressure was the rapid combustion of the hydrogen in the combustion chamber, and the pressure spikes were from the pressure waves colliding throughout the chamber.

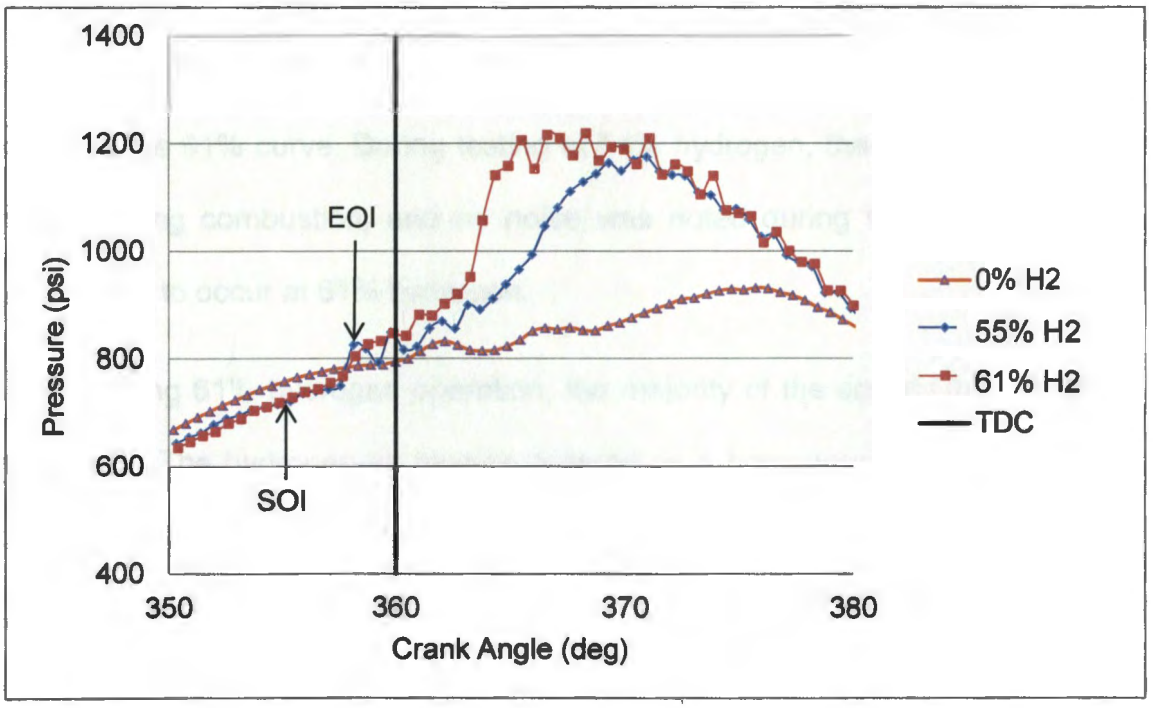

Figure 17: Pressure curves analyzed for knock at 1300 RPM.

The 54% pressure curve exhibited a couple of pressure spikes prior to TDC. The 61% hydrogen pressure curve also experienced short, rapid pressure increases, but the pressure did not drop down and create a noticeable spike as seen in the 54% hydrogen pressure curve. In both the 54% and 61% hydrogen experiments, the pressure spikes/rapid increase were possibly from the end of injection (EOI) of the primary injection, the self-ignition of the pilot injection, or a combination of both. The start of injection (SOI) and EOI are included for the

primary injection. For both the 54% and 61% hydrogen experiments, the SOI and EOI occurred at 5 deg BTDC and 3 deg BTDC, respectively. The injection timing was included to determine if fuel injection aided in creating pressure spikes characteristic of knock. The fuel injection was finished prior to the rapid combustion and did not contribute to pressure spikes occurring between 365-375 deg. The pressure rise from combustion in the 54% pressure curve was not as steep as the 61% curve. During testing at 54% hydrogen, there were no pressure spikes during combustion, and no noise was noted during testing. Knock was determined to occur at 61% hydrogen.

During 61% hydrogen operation, the majority of the energy input was from hydrogen. The hydrogen-air mixture entered as a homogenous charge ready for combustion. With the diesel being used as the ignition source, multiple ignition sites occurred as expected in typical diesel combustion. The rapid pressure rise was the initial combustion of the hydrogen-air mixture followed by the collision of flame fronts. As mentioned in the background, knock in a diesel engine occurs when too much fuel is ready to combust at the time that self-ignition occurs. That results in the 'rapid' pressure rise [12]. The collision of flame fronts was a source of the pressure spikes during knock.

The ECM changed the injection timing of the diesel fuel as more hydrogen was added. The expected change was to retard the injection to account for the faster burn rate of hydrogen. The ECM advanced the injection as more hydrogen was added. Figure 18 shows the injection change as hydrogen was increased.

The pilot injection advanced more than the primary injection. The original purpose of the pilot injection was twofold. It made the engine run smoother, and it reduced emissions of PM, HC, and CO.

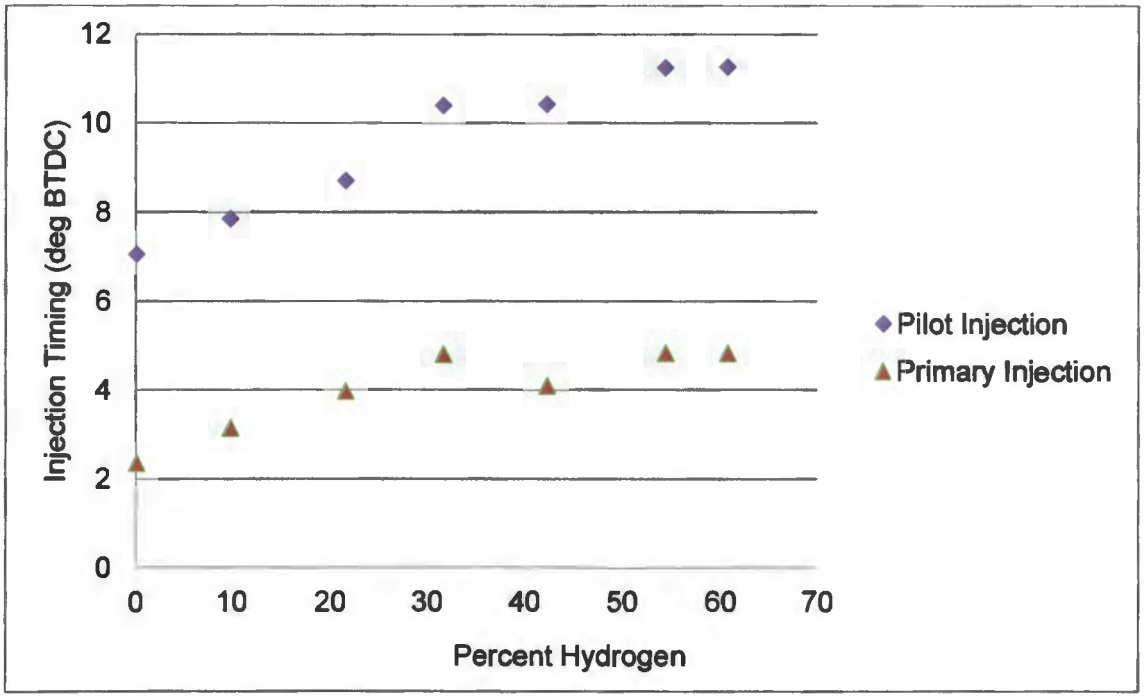

Figure 18: Injection change as hydrogen increased for 1300 RPM.

The early pilot injection allowed time for the fuel preparation to occur. As self-ignition of the pilot injection was occurring, the primary injection was starting. The high temperatures from the start of ignition aided in the rapid preparation of the primary injection for combustion. The combustion of the pilot injection resulted in a slower, more controlled pressure rise.

As hydrogen was added, the pilot injection occurred sooner. The control algorithm used within the ECM was proprietary information, and the inputs used to change the injection timing were not known. The predicted inputs used to sense

the addition of hydrogen, which in turn changed the injection timing, were the crankshaft speed sensor and the fuel pump speed sensor. The ECM would likely compare the crankshaft speed sensor to the fuel pump speed sensor and detect slight differences. The ECM likely had a threshold for the crankshaft and fuel pump speed differences which were exceeded during dual fuel combustion. The dual fuel combustion was possibly interpreted as engine knock. By separating the pilot injection from the primary injection, more time was allowed for self-ignition. With more time for self-ignition to occur, an excess of fuel was not ready for combustion. Hence, there would be a slower, more controlled pressure rise. Figure 18 shows the separation of the pilot injection and primary injection timing that the ECM would be expected to do based upon interpreting engine knock.

The pressure curves for 1800 RPM are presented in Figure 19. This group of pressure curves was not like the pressure curves from the 1300 RPM test because the ECM changed the amount of boost. There was no gradual increase in peak pressure like 1300 RPM. It remained roughly constant except for when 66% hydrogen was used. Instead of an increase in peak pressure, a gradual increase in pressure around 380 degrees crank angle occurred. This is shown in Figure 19 with the arrow labeled 'Increasing hydrogen'. That increase resulted in the pressure curves exhibiting characteristics more like a Diesel Cycle (constant pressure) than an Otto Cycle (constant volume). As that occurred, the SEC increased.

The rapid pressure rise associated with hydrogen-air combustion was not particularly noticeable until 46% hydrogen addition. The SEC started decreasing at 46% hydrogen and continued decreasing as more hydrogen was added. The rapid combustion of the hydrogen-air mixture helped decrease the SEC by shifting combustion characteristics towards an SI engine.

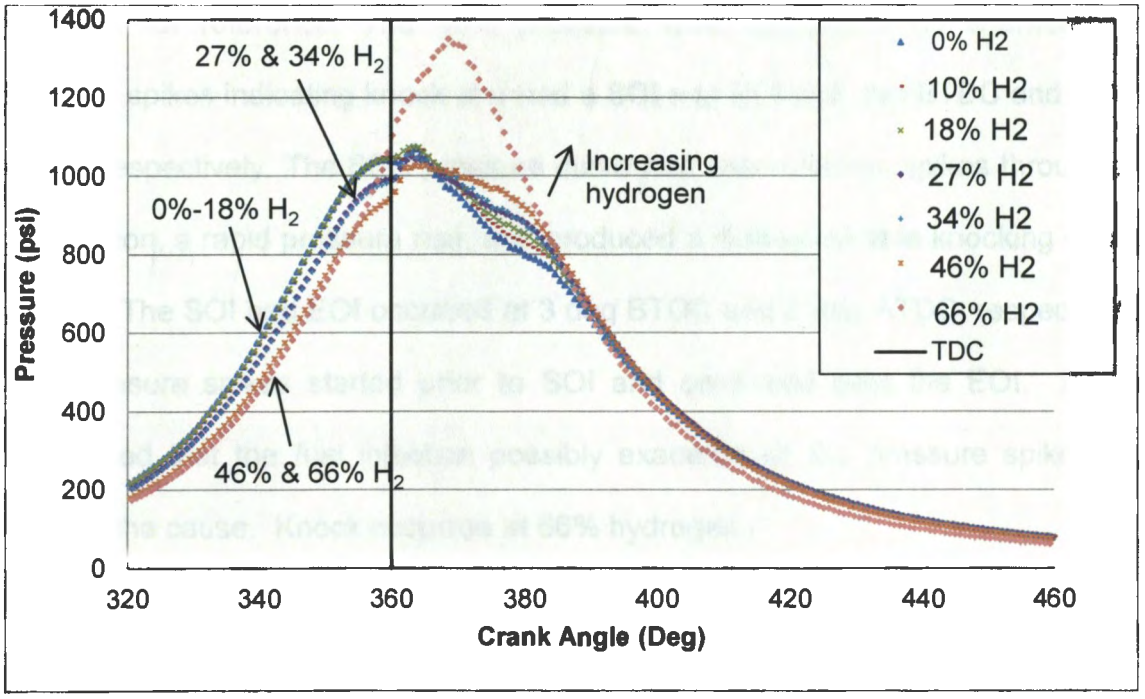

Figure 19: Pressure curves for 1800 RPM with varying percentages of hydrogen.

As the percentage of hydrogen increased, several different profiles of pressure curves resulted. The first profile included 0%-18% hydrogen. The next profile included pressure curves 27% and 34%. The 46% and 66% started with the same profile but separated once combustion started. The different profiles occurred because different levels of boost were used. The pressure curves illustrated that the ECM decreased boost as hydrogen was added. This was

recognized by the profile groups having a lower pressure at the same crank angle prior to TDC.

Similar to the 1300 RPM test, the 66% and 46% hydrogen pressure waves were examined for indication of knock and the injection timing was included. Figure 20 shows those pressure curves along with the baseline pressure curve (0% H_2), for reference. The 46% pressure wave contained no characteristic pressure spikes indicating knock and had a SOI and EOI at 2 deg BTDC and 7 deg ATDC, respectively. The 66% pressure curve had characteristic spikes throughout combustion, a rapid pressure rise, and produced a distinguishable knocking sound as well. The SOI and EOI occurred at 3 deg BTDC and 2 deg ATDC, respectively. The pressure spikes started prior to SOI and continued past the EOI. It was determined that the fuel injection possibly exacerbated the pressure spikes but was not the cause. Knock occurred at 66% hydrogen.

The ECM changed the boost and injection timing as hydrogen was added during the 1800 RPM test. Similar to the 1300 RPM, the injection timing was advanced as hydrogen was added. The injection changes are shown in Figure 21. The pilot and primary injection diverged as hydrogen was added. Aside from the injection changes, the boost was decreased. The boost was decreased to control the start of ignition. Diesel fuel ignites at a specific temperature and pressure. The higher pressure from the turbocharger and the faster combustion from the hydrogen resulted in peak pressure occurring closer to TDC. The ECM decreased the boost to delay ignition and the timing of peak pressure.

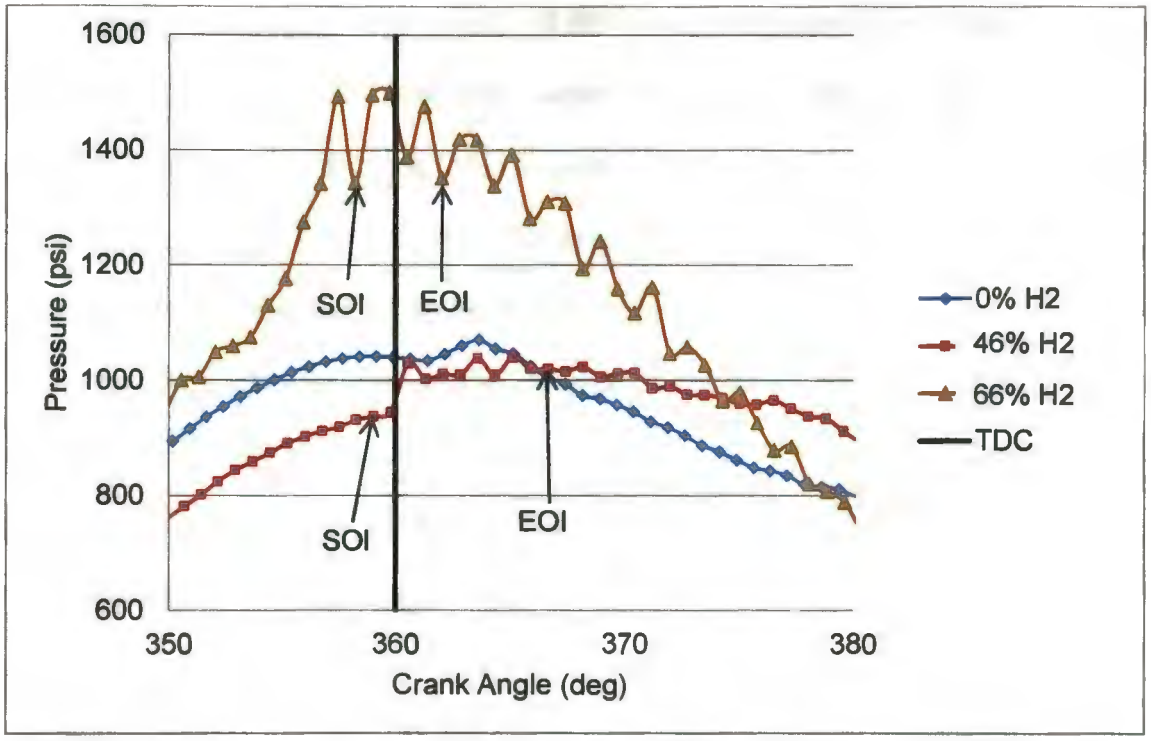

Figure 20: Pressure curves analyzed for knock at 1800 RPM.

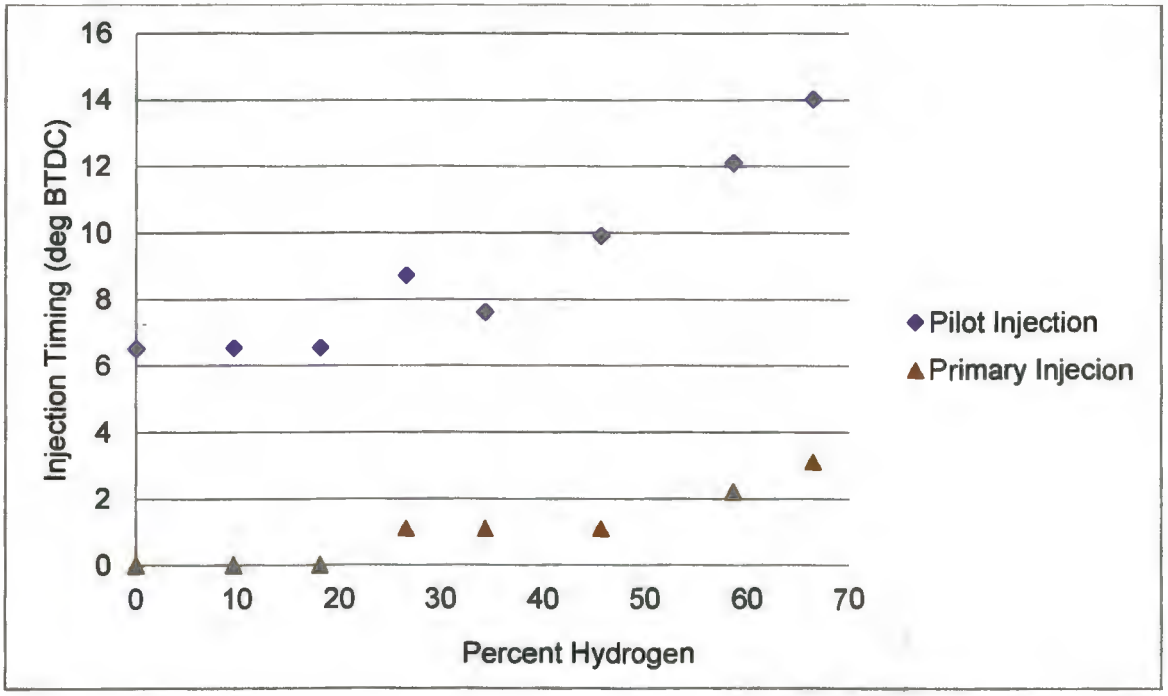

Figure 21: Injection change as hydrogen increased for 1800 RPM.

The pressure curves for the 2100 RPM test are presented in Figure 22. The results from the 2100 RPM test speed were similar to the results from the 1800 test speed. There was one group of pressure curves operating at the same level of boost which were 0% and 10% hydrogen. As hydrogen increased, all the other pressure curves operated at lower levels of boost. The arrow labeled 'Increasing hydrogen' in Figure 22 shows the change in pressure curves. The pressure curves for 0%-36% hydrogen all had a gradual reduction in pressure charge and general decrease in peak pressure. The SEC experienced an increase throughout this hydrogen operating range. The faster combustion from hydrogen addition, which decreased SEC, was counteracted by the decrease in pressure. This resulted in a higher SEC. At 55% hydrogen, the rapid combustion of hydrogen increased the cylinder pressure enough to overcome the decrease in pressure charge and produce a decrease in SEC. Likewise, at 65% hydrogen, the same results occurred.

The 55% and 65% pressure curves were examined for knock. They are shown in Figure 23 along with the baseline pressure curve and the fuel injection timing. The SOI and EOI were 5 deg BTDC and 4 deg ATDC, respectively, for 55% hydrogen, and for 65% hydrogen, the SOI and EOI were 7 deg BTDC and 1 deg ATDC, respectively. Both curves had the same rapid pressure increase at the start of combustion which is characteristic of knock. The 55% hydrogen pressure curve did not have pronounced pressure spikes characteristic of knock, but the 65% hydrogen pressure curve had several pressure spikes during combustion. The pressure spikes, which occurred during the 65% hydrogen experiment, may

have been influenced by the fuel injection, so they were not considered a determining factor for knock. The largest differentiation between the 55% and 65% hydrogen test conditions for knock detection was the distinctive noise. The 55% hydrogen operating state did not have the characteristic sound, so it was determined that knock was not occurring. At 65% hydrogen, the characteristic knock sound was audible; thus, knock was determined to be present.

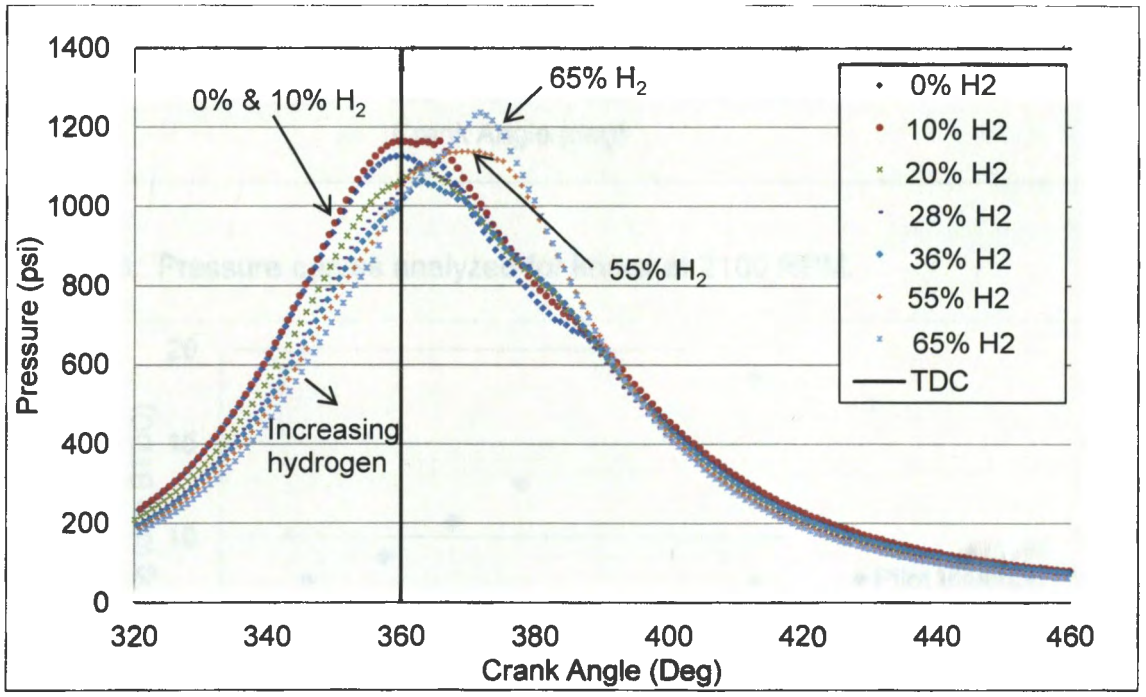

Figure 22: Pressure curves for 2100 RPM with varying percentages of hydrogen.

Similar to the 1800 RPM operating condition, the 2100 RPM test varied the boost and the injection timing as hydrogen was added. The boost was decreased to control the start of ignition, and the injection timing was advanced for smoother engine operations. The injection advance, as hydrogen was added, is shown in Figure 24.

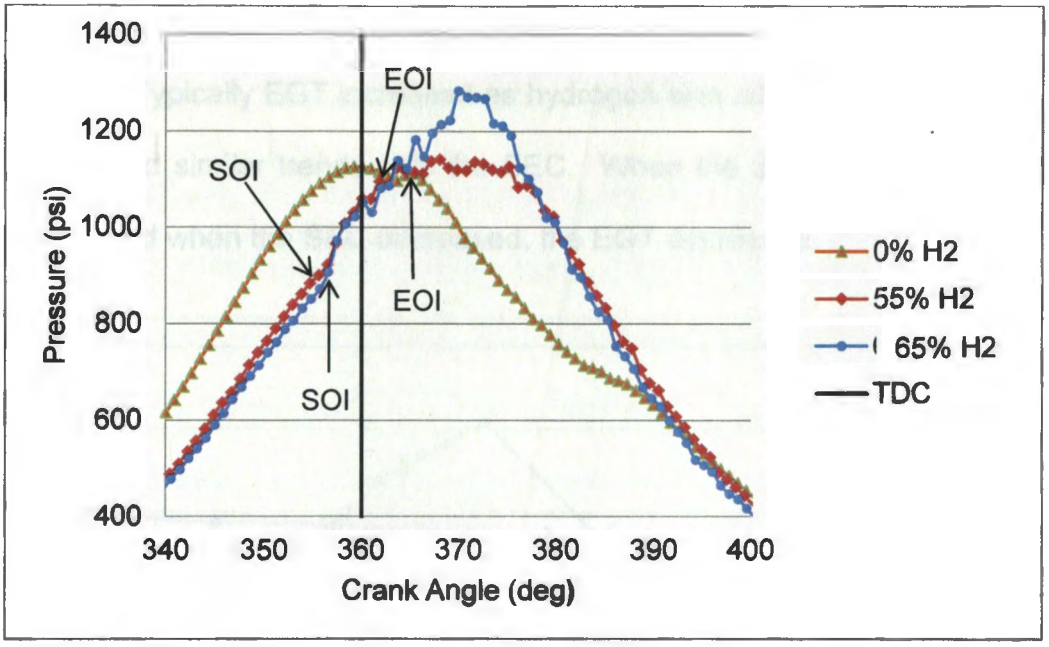

Figure 23: Pressure curves analyzed for knock at 2100 RPM.

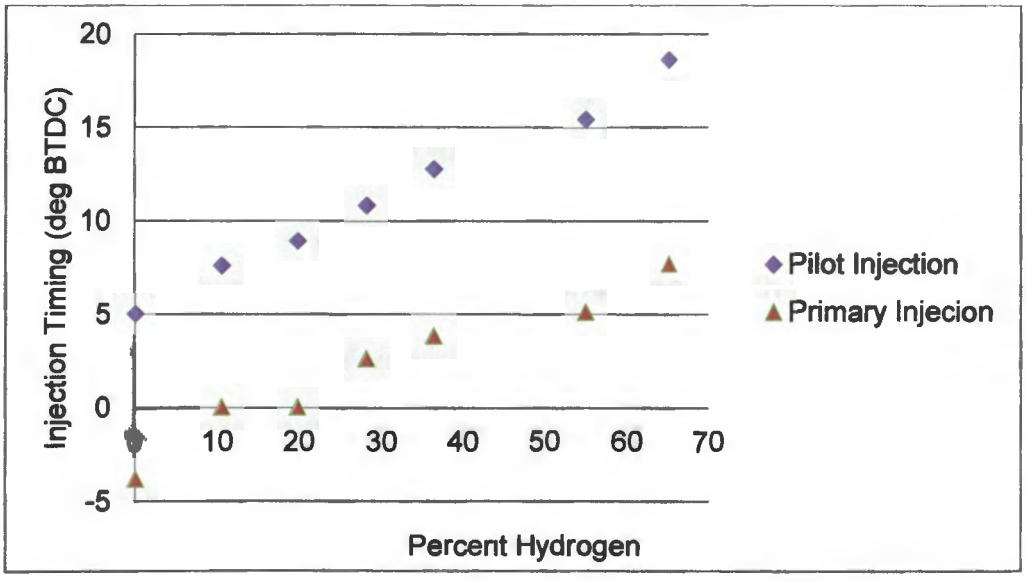

Figure 24: Injection change as hydrogen increased for 2100 RPM.

The EGT for all operating speeds are shown in Figure 25. During testing, the intake charge was maintained at 130°F for all test speeds. This value was chosen because it was the temperature used for testing according to the CAT

specifications sheet. The EGT results were not consistent with other research [36, 37, 43, 46]. Typically EGT increased as hydrogen was added. During testing, the EGT displayed similar trends with the SEC. When the SEC increased, the EGT increased, and when the SEC decreased, the EGT decreased.

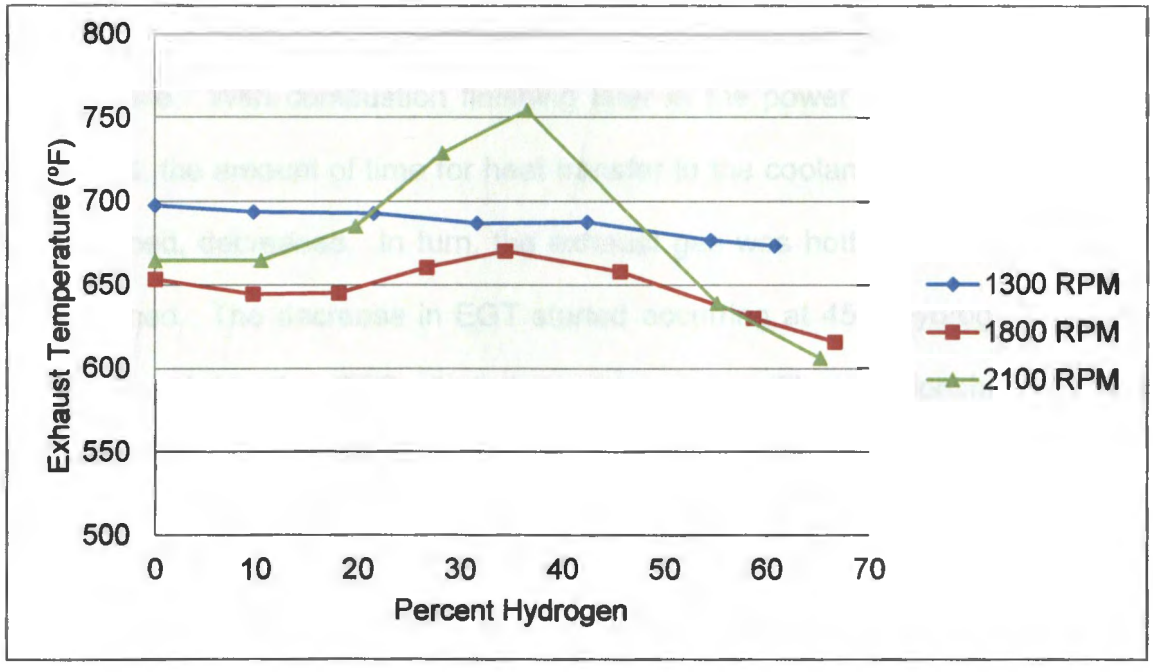

Figure 25: Exhaust temperatures for all operating speeds with hydrogen addition.

The EGT for 1300 RPM experienced a linear decrease as hydrogen was added. This was similar to the linear decrease in SEC. The addition of hydrogen resulted in combustion occurring sooner and faster. The combustion process behaved more like an SI engine combustion process (constant volume). This faster combustion increased the amount of time for heat transfer through the cylinder head and engine block, to the engine coolant, before the exhaust valve opened. Once the exhaust valve opened, the hot exhaust gas rapidly exited the

combustion chamber. The increasing amount of time for heat transfer, as hydrogen was added, resulted in lowering the EGT as hydrogen was added.

The EGT and SEC exhibited similar trends at 1800 RPM. The increase in SEC at 1800 resulted because the combustion process behaved like a CI engine (constant pressure). The constant pressure combustion continued longer into the power stroke. With combustion finishing later in the power stroke, as hydrogen was added, the amount of time for heat transfer to the coolant, before the exhaust valve opened, decreased. In turn, the exhaust gas was hotter when the exhaust valve opened. The decrease in EGT started occurring at 45% hydrogen addition which was where the SEC started to decrease. (The relationship between decreasing SEC and EGT was explained previously in this paper.)

The EGT for 2100 RPM varied the most during hydrogen addition. The EGT increased while the SEC increased and decreased while the SEC decreased. The increasing trend, however, was different. The SEC had a slight linear increase up to 36% hydrogen, whereas the EGT experienced a larger increase up to 36% hydrogen. The larger increase in EGT, compared to 1800 RPM, was expected to result from the increased operating speed during the 2100 RPM test. The higher engine speed decreased the time for heat transfer and so did the constant pressure combustion associated with the increase in SEC. As combustion continued longer into the power stroke, which was occurring faster, less heat was removed from the exhaust via heat transfer to the engine coolant. This resulted in

a larger increase in EGT compared to 1800 RPM. The decrease in EGT coincides with the decrease in SEC, which was explained previously.

6.3. Emissions

The results for the variation of HC emissions during all test speeds are presented in Figure 26. The HC emissions do not vary from 1 PPM except for two instances. Testing conducted using the same equipment had HC emissions vary between 1 and 3 PPM [38]. The lack of variation in two studies raised concern that the HC meter might be faulty. An experiment was conducted after the hydrogen testing to verify if the HC meter was working. The exhaust gas analyzer was used to monitor the HC emissions from a two-stroke snowmobile engine. An operating characteristic of two-stroke engines is to have unburnt HC emissions in their exhaust [12]. Because of the known HC emissions, the exhaust gas analyzer was expected to have a reading other than 1 or 2 PPM. The two-stroke engine test had HC emissions ranging from 260-270 PPM. This verified that the HC meter was working, but it did not verify the calibration was still accurate during testing.

Because of the uncertainty of the calibration, the general trend in HC emissions was examined Based upon the HC emission results from testing at different operating speeds, it was concluded that hydrogen addition did not affect HC emission. The addition of hydrogen did not improve upon the completeness of combustion achieved by the ACERT ECM. For comparison of HC emissions, other research found HC emissions were reduced from 19 PPM at baseline to 3 PPM during hydrogen addition on an engine which did not use common rail fuel delivery.

That engine used a mechanical fuel injection system with an injection pressure of 240 bar [37]. The use of a common rail fuel delivery system has been shown to reduce HC emissions compared to mechanical fuel injection systems [27,33]. The HC emissions results seem accurate compared to previous published results because the common rail fuel system and ACERT ECM are expected to reduce emissions compared to mechanical fuel injection systems.

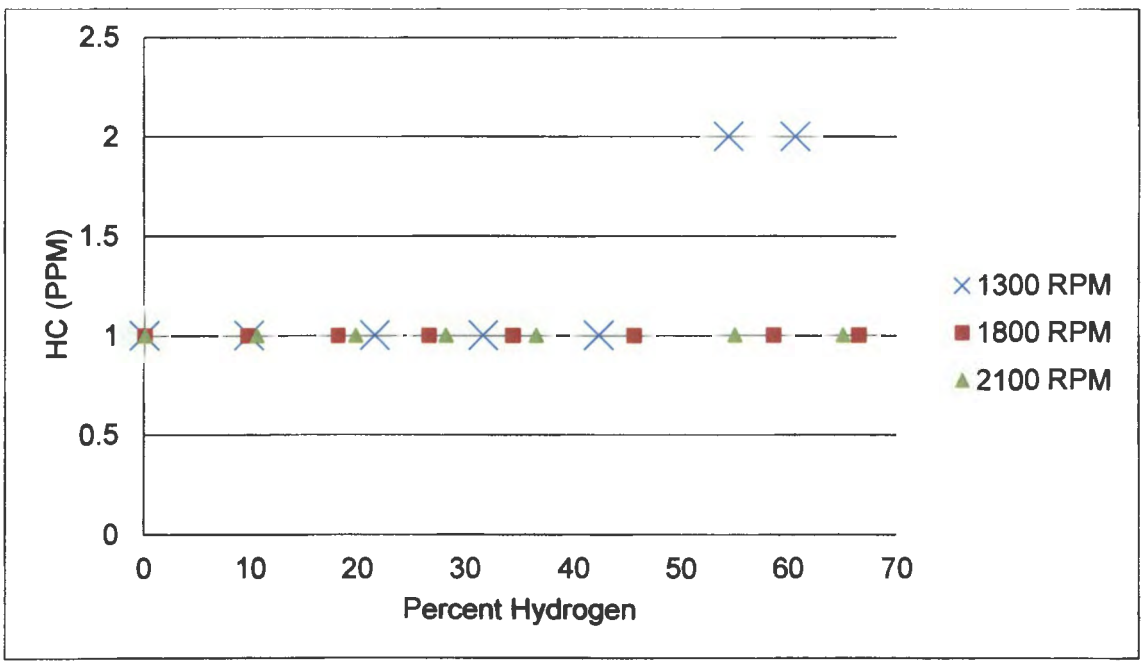

Figure 26: Variation of HC emissions for all test speeds.

The results for CO emissions, during all test speeds, are presented in Figure 27. The 1300 CO emission started at 0.03%. It decreased to 0.02% when 42% hydrogen was added, and it remained there as hydrogen was increased. The decrease in CO results from consistent combustion and a decrease in the carbon input. The 1800 RPM test had an increase in CO that coincides with the increase in SEC. The increase in SEC resulted from the decrease in combustion efficiency.

The decrease at higher percentages of hydrogen occurred because of the decrease in carbon input. The 2100 RPM test had similar results as the 1800 RPM for the same reasons. The ability to use hydrogen as an alternative fuel, with the CAT ACERT ECM, reduced CO emissions by reducing the input of carbon.

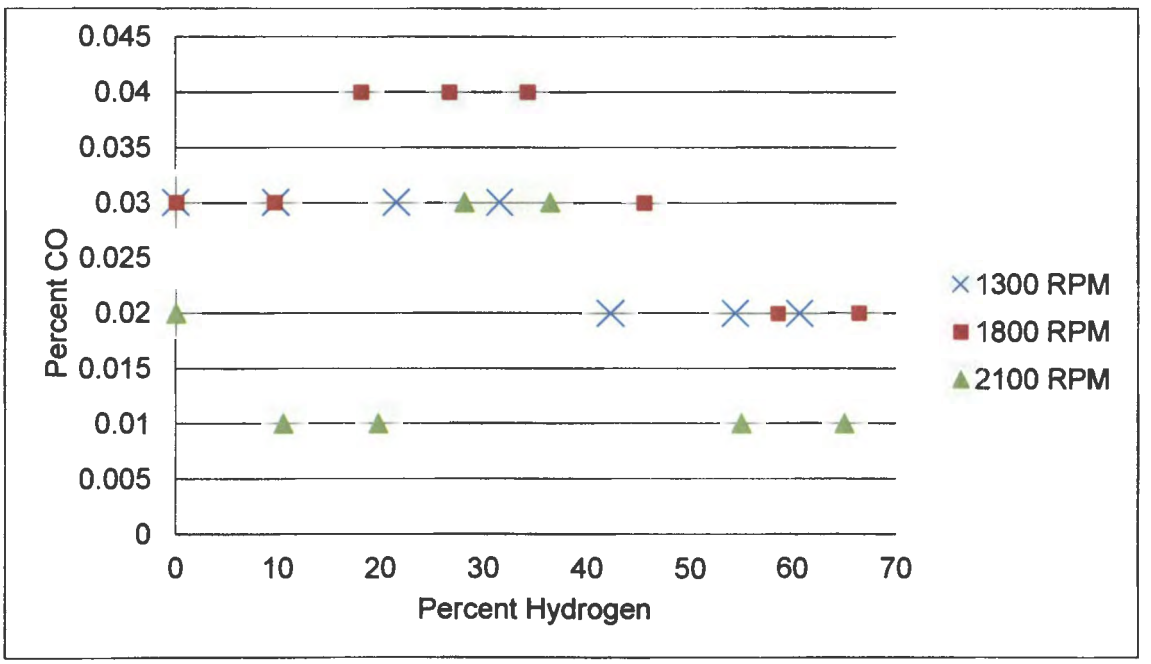

Figure 27: Variation of CO emissions for all test speeds.

The variation of CO_2 emissions, for all test speeds, is shown in Figure 28. Included in Figure 28, is the decrease in diesel fuel consumption for all test speeds. The diesel fuel consumption values were scaled to replicate the CO_2 emissions layout. All test speeds experienced a decrease in CO_2 emissions. The decrease in carbon input resulted in the decrease. The diesel fuel consumptions were included to show the relationship between the decrease in diesel input and reduction in CO_2 emissions. The reduction in CO_2 correlates with the reduction in diesel fuel consumption. For all test speeds, the slopes are approximately the

same. The ability to use hydrogen as an alternative fuel, with the CAT ACERT ECM, reduced CO_2 emissions by reducing the input of carbon.

The variation of NO_x emissions is shown in Figure 29. Across all test speeds, an increase in NO_x emissions occurred. Increased NO_x emissions are usually associated with higher EGT. For the 1300 RPM test, the EGT did not increase, yet there was an increase in NO_x emissions.

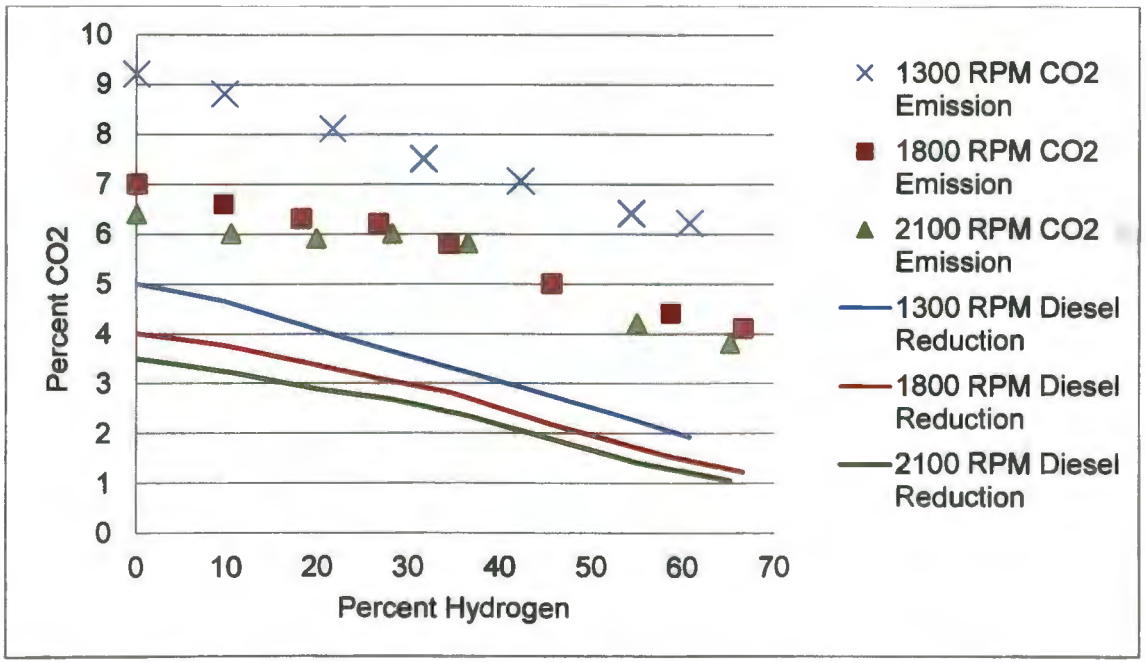

Figure 28: Variation of CO_2 emissions for all test speeds.

The implementation of hydrogen resulted in faster combustion. This, in turn, made a faster temperature rise. The combustion reactants experienced a longer residence time in the combustion chamber at the elevated temperature. The injection advances also increased the residence time which aided in increasing the NO_x emissions. NO_x formation is not only dependent on combustion temperatures,

but also on injection timing [46]. A decrease in NO_x resulted from retardation of the injection timing, but increased the SEC [46]. The injection advance, dictated by the ACERT ECM, increased NO_x emissions. The ability to retard the injection timing for the CAT engine, while adding hydrogen, would potentially prevent an increase in NO_x emissions.

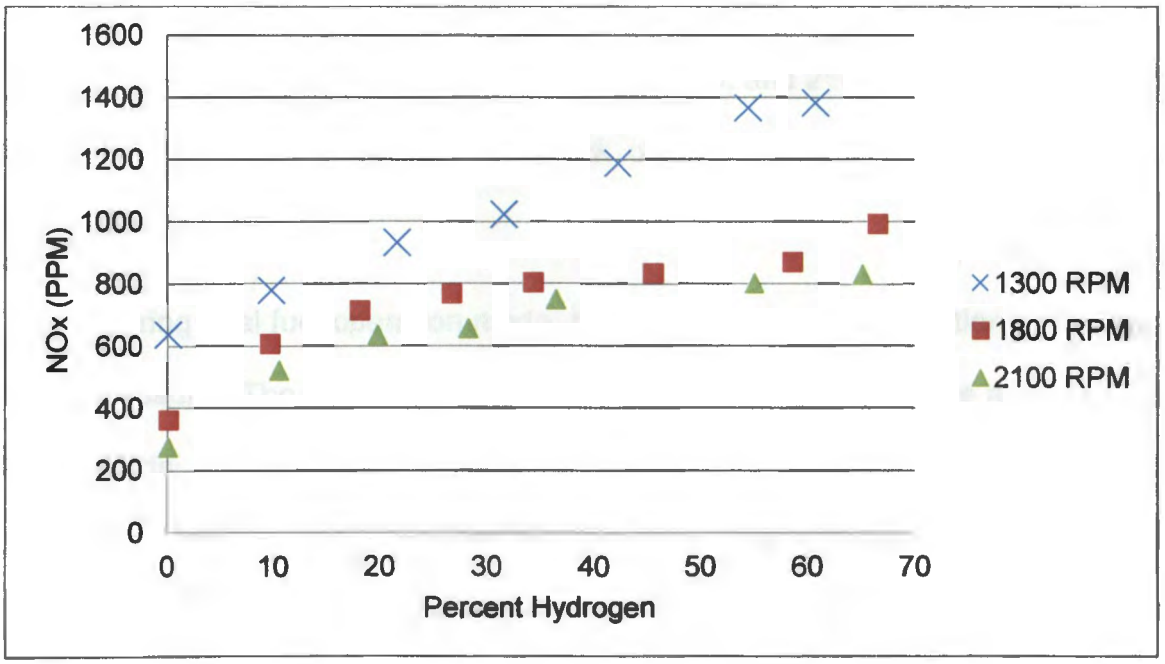

Figure 29: Variation of NO_x emissions for all test speeds

CHAPTER 7. CONCLUSION

The primary objective of this study was to determine the capability of a CAT engine controlled by an ACERT ECM to operate in dual fuel mode. Because the CAT test engine was successfully operated in dual fuel mode, it was concluded that a CAT engine controlled by an ACERT ECM can operate in dual fuel mode. It can be operated from approximately 0-50% hydrogen before knock occurs. At 50% of rated load, and at test speeds of 1300, 1800, and 2100 RPM, the maximum amount of hydrogen added before knock occurred was 54%, 46%, and 55%, respectively.

During dual fuel operation mode, the ECM adjusted the injection timing and boost pressure. The injection timing was advanced as hydrogen was added for all test speeds. The injection timing was modified for smoother combustion and operation. The boost was reduced at 1800 and 2100 RPM to control the start of ignition. The ECM changes allowed the engine to operate efficiently in dual fuel mode. At 1300 RPM, hydrogen addition resulted in a decrease in SEC. For 1800 and 2100 RPM, the SEC improved only when hydrogen was added beyond 46% and 55% energy, respectively. Operation at these levels of hydrogen placed combustion close to the knock operation limit.

Emissions testing, while using hydrogen, showed a consistent increase in NO_x emissions for all test speeds. The CO emissions showed improvement at levels of hydrogen exceeding 40% energy for all test speeds. The CO_2 emissions decreased for all levels for hydrogen. The ability to use hydrogen as an alternative

fuel reduced the carbon input which in turn helped reduce the CO and CO_2 emissions. The HC emissions trend appeared to be unaffected by hydrogen addition. The ACERT ECM fuel injection control produced complete combustion, upon which hydrogen addition did not improve. The lack of variation in the HC emissions raised the concern that the sensor might be broken. Additional testing verified the sensor was working but did not verify if the sensor was still properly calibrated. Based on previous published results, the HC emissions values are not unreasonable.

7.1. Future Work

Future work focusing on reducing the NO_x emissions would yield improvements when operating in dual fuel mode. Retarding injection timing would be expected to yield improvements in NO_x emissions based off previous research [46]. The ability to control injection timing requires access to the ACERT ECM, or the implementation of an aftermarket ECM. With access to the ECM, control strategies can be modified to increase the level of hydrogen addition before knock limits engine operation. The ability to use higher percentages of hydrogen would be expected to yield further decreases in CO and CO_2 emissions. A recalibration of the exhaust gas analyzer would increase the confidence in future emissions results.

REFERENCES CITED

[1] U.S. Energy Information Administration, 2010, "Annual Energy Review 2009," from http://205.254.135.24/totalenergy/data/annual/pdf/aer.pdf

[2] Organization of the Petroleum Exporting Countries, 2010, "World Oil Outlook," from http://www.opec.org/opec_web/static_files_project/media/downloads/publications/WOO_2010.pdf

[3] US Energy Information Administration, 2010, "International Energy Outlook 2010," from http://205.254.135.24/oiaf/ieo

[4] Almedia, P. and Silva, P., 2009, "The Peak of Oil Production - Timing and Market Recognition," Energy Policy, **37,** pp. 1267-1276.

[5] Hirsch R., Bezdek R., and Wendling R., 2005, "Peaking of World Oil Production: Impacts, Mitigation, and Risk Management," from http://www.netl.doe.gov/energy-analyses/pubs/Oil_Peaking_NETL.pdf

[6] Roper, D., 2011, "World Fossil-Fuels Depletion," from, http://www.roperld.com/science/minerals/fossilfuels.htm.

[7] Environmental Protection Agency, 2011, "Air pollution Emission Overview," from http://www.epa.gov/oaqps001/emissns.html

[8] Environmental Protection Agency, 2009, "1970-2008 Average Annual Emissions," from http://www.epa.gov/ttnchie1/trends

[9] Australian Government: Department of Sustainability, Environment, Water, Population and communities, 2006, "Indicator: A-32 Implementation of National Fuel Quality Standards," from http://www.environment.gov.au/soe/2006/publications/drs/indicator/373/index.html

[10] Canadian Council of Ministers of the Environment, 2011, "What is Smog," from http://www.ccme.ca/assets/pdf/pn_1257_e.pdf

[11] Committee on Alternatives and Strategies for Future Hydrogen Production and Use, National Research Council, and National Academy of Engineering, 2004, "The Hydrogen Economy: Opportunities, Costs, Barriers, and R&D Needs," National Academy Press.

[12] Stone, R., 1999, *Introduction to Internal Combustion Engines*, 3rd ed., Society of Automotive Engineers, Inc., Warrendale PA.

[13] The Web's Where You Study In, 2008, "Four Stroke Engine," from

http://www.ustudy.in/node/3268

[14] Sonntag R. E., Borgnakke, C. and Van Wylen G. J., 2003, *Fundamentals of Thermodynamics*, 6th ed., John Wiley and Sons.

[15] Taylor B., 2009, "Turbos in Car Engines," from http://engineerography.com/2009/04/turbos-in-car-engines/

[16] Pulkrabek, W., 2004, *Engineering Fundamentals of the Internal Combustion Engine*, 2nd ed., Pearson Prentice-Hall.

[17] Nordin, N., n.d., "Introduction to Combustion in Diesel Engines," from http://files.nequam.se/greenCarLecture.pdf

[18] Verhelst, S. and Wallner, T., 2009, "Hydrogen-fueled Internal Combustion Engines," Progress in Energy and Combustion Science, **35**, pp. 490-527.

[19] Heywood, J. and Vilchis, F., 1984, "Comparison of Flame Development in a Spark-Ignition Engine Fueled with Propane and Hydrogen," Combustion Science Technology, **38**, pp. 313-324.

[20] Cambel, A. B. and Jennings B. H., 1958, *Gas Dynamics*, McGraw-Hill, New York.

[21] Amann, C., 1985, "Cylinder Pressure Measurement and Its Uses in Engine Development," 0148-7191/85/1021-2067, Society of Automotive Engineers Inc., Warrendale PA.

[22] Martyr, A. and Plint, M., 2007, *Engine Testing*, 3rd ed., Society of Automotive Engineers Inc., Warrendale, PA.

[23] Environmental Protection Agency, 2011, "Fuels and Engines," from http://www.epa.gov/agriculture/fuel.html

[24] Webster, L., 2009, "The Future of Diesel in the US," from http://www.popularmechanics.com/cars/alternative-fuel/diesel/4330313

[25] US Department of Energy, 2009, "Diesel Car Sales in Europe Still over 50% in 2008," from http://www1.eere.energy.gov/vehiclesandfuels/facts/2009_fotw575.html

[26] Worldometer, 2011, "Cars Produced This Year," from http://www.worldometers.info/cars/

[27] John Deere, 2007, "Emissions Technology Brochure"

[28] Moore, W., 2003, "Living with cooled-EGR engines," Construction equipment, pp. 68-69.

[29] Zheng, M., Reader, G. and Hawley, J. G., 2004, "Diesel Engine Exhaust Gas Recirculation- A Review on Advanced and Novel Concepts," Energy Conversion and Management, **45,** pp. 883-900.

[30] Filipi, Z., Wang, Y. and Assanis, D., 2001, "Effect of Variable Geometry Turbine (VGT) on Diesel Engine and Vehicle System Transient Response," 2001-01-1247, Society of Automotive Engineers Inc., Warrendale, PA.

[31] Facts about SCR, 2008, "SCR Environmental Advantage," from http://www.factsaboutscr.com/environment/default.aspx

[32] Tomoda, T. et al., 2010, "Improvement of Diesel Engine Performance by Variable Valve Train System," International Journal of Engine Research, **11,** pp. 331-344.

[33] Brownlee, J., 2005, "Common rail fuel injection," from http://www.marlinmag.com/common-rail-fuel-injection

[34] Ozsezen, A., Canakci, M., Turkcan, A. and Sayin, C., 2008, "Performance and Combustion Characteristics of a DI Diesel Engine Fueled with Waste Palm Oil and Canola Methyl Esters," Fuel, **88** pp. 629-636.

[35] Saravanan, N. and Nagarajan, G., 2008, "An Experimental Investigation of Hydrogen-Enriched Air Induction in a Diesel System," International Journal of Hydrogen Energy, **33**, pp. 1769-1775.

[36] Bose, P. and Maji, D., 2009, "An Experimental Investigation on Engine Performance and Emissions of Single Cylinder Diesel Engine Using Hydrogen as Inducted Fuel and Diesel as Injected Fuel with Exhaust Gas Recirculation," International Journal of Hydrogen Energy, **34**, pp. 4847-4854.

[37] Saravanan, N., Nagarajan, G., Dhanasekaran, C. and Kalaiselvan, K., 2007, "Experimental Investigation of Hydrogen Port Fuel Injection in DI Diesel Engine," International Journal of Hydrogen Energy, **32**, pp. 4071-4080.

[38] Stousland, T., Work in Progress, "Experimental Use of Hydrogen to Reduce the Consumption of Carbon Fuels in a Compression Ignition Engine and its Effects on Performance," M.S. Thesis, Mechanical Engineering Department,

North Dakota State University.

[39] Gomes Antunes, J., Mikalsen, R. and Roskilly, A., 2009, "An Experimental Study of a Direct Injection Compression Ignition Hydrogen Engine," International Journal of Hydrogen Energy, **34,** pp. 6516-6522.

[40] Szwaja, S. and Grab-Rogalinski, K., 2009, "Hydrogen Combustion in a Compression Ignition Diesel Engine," International Journal of Hydrogen Energy, **34**, pp. 4413-4421.

[41] Saravanan, N. and Nagarajan G., 2009, "Performance and Emission Study in Manifold Hydrogen Injection with Diesel as an Ignition Source for Different Start of Injection," Renewable Energy, **34,** pp. 328-334.

[42] Saravanan, N. et al., 2008, "Combustion Analysis on a DI diesel Engine with Hydrogen in Dual Fuel Mode," Fuel, **87**, pp. 3591-3599.

[43] Shirk, M., McGuire, T., Neal, G. and Haworth, D., 2008, "Investigation of a Hydrogen-Assisted Combustion System for a Light-Duty Diesel Vehicle," International Journal of Hydrogen Energy, **33,** pp.7237-7244.

[44] Gatts, T. et al., 2010, "An Experimental Investigation of H_2 Emissions of a 2004 Heavy-Duty Diesel Engine Supplemented with H_2," International Journal of Hydrogen Energy, **35**, pp. 11349-11356.

[45] National Academy of Science, 2008, "Understanding and Responding to Climate Change," from http://dels-old.nas.edu/dels/rpt_briefs/climate_change_2008_final.pdf

[46] Lilik, G. et al., 2010, "Hydrogen Assisted Diesel Combustion," International Journal of Hydrogen Energy, **35**, pp. 4382-4398.

[47] Caterpillar Inc., 2005, "Built for the Next Generation: CAT Tier 4 Interim/ Stage IIIB Technologies," from http://www.cat.com/cda/files/2414946/7/Tier_4-_Engine_value_brochure.pdf on August 15 2011.

APPENDIX A. SAMPLE DATA SPREADSHEETS

Table 2: DYNOmite-Pro data spreadsheet sample.

Load, CFM	Absorber RPM-C	Fuel Flow	Torque	H2 Flow	Barometer	Humidity
50% 0	2099.621	5.255	223.002	0.052	14.346	65.102
50% 3.7	2110.213	4.837	220.459	0.155	14.346	63.722
50% 7.3	2119.802	4.339	221.386	0.249	14.346	63.232
50% 11	2124.783	4.014	223.979	0.345	14.346	63.461
50% 14.3	2129.006	3.523	226.163	0.428	14.346	62.629
50% 18.3	2143.070	2.120	225.614	0.536	14.346	64.150
50% 20.8	2146.200	1.582	228.258	0.602	14.345	64.216
Board Time	**Absorber RPM-C**	**Fuel Flow**	**Torque**	**H2 Flow**	**Barometer**	**Humidity**
0.000	2110.000	4.845	209.835	0.052	14.346	65.492
0.504	2087.000	5.010	228.144	0.052	14.346	65.492
1.008	2088.000	5.247	228.293	0.053	14.346	65.489
1.512	2106.000	5.480	219.504	0.052	14.346	65.476
2.016	2108.000	5.227	217.763	0.053	14.346	65.473
2.519	2092.000	5.090	229.620	0.053	14.347	65.460
3.021	2088.000	5.376	232.240	0.052	14.346	65.432
3.525	2105.000	5.436	220.731	0.052	14.347	65.414
4.029	2108.000	5.259	216.983	0.052	14.346	65.388
4.533	2098.000	5.094	227.630	0.052	14.346	65.388
5.037	2089.000	5.223	232.041	0.052	14.346	65.377
5.541	2103.000	5.492	220.283	0.052	14.346	65.379
6.043	2108.000	5.327	217.928	0.052	14.346	65.382
6.545	2103.000	5.066	224.761	0.051	14.346	65.396
7.049	2088.000	5.223	232.091	0.052	14.346	65.412
7.549	2100.000	5.508	222.041	0.052	14.346	65.429
8.052	2108.000	5.364	220.018	0.051	14.346	65.455
8.556	2104.000	5.147	222.854	0.053	14.346	65.469
9.060	2086.000	5.151	230.748	0.052	14.346	65.476
9.564	2097.000	5.548	226.403	0.052	14.346	65.478
10.068	2109.000	5.380	220.383	0.052	14.347	65.476
10.572	2106.000	5.115	217.447	0.052	14.346	65.449
11.076	2086.000	5.127	232.472	0.052	14.346	65.412
11.580	2093.000	5.552	227.613	0.052	14.346	65.364
12.084	2108.000	5.476	220.698	0.051	14.346	65.304
12.588	2107.000	5.207	218.575	0.056	14.346	65.254
13.092	2089.000	5.094	231.660	0.115	14.346	65.196
13.596	2091.000	5.488	230.764	0.060	14.346	65.159
14.100	2106.000	5.408	220.416	0.052	14.346	65.124
14.603	2110.000	5.231	216.452	0.050	14.346	65.081
15.107	2095.000	5.070	230.018	0.049	14.346	65.049
15.609	2091.000	5.315	231.046	0.051	14.346	65.025
16.113	2107.000	5.496	219.753	0.051	14.346	64.997

Table 2 (continued)

EGT #1	EGT #2	EGT #4	EGT #5	EGT #8	Air Temp.	Air Flow	%H2 Energy
664.356	521.183	216.286	57.367	78.709	80.000	345.972	0.00
664.444	523.010	217.987	57.399	69.434	80.557	345.720	10.49
684.845	549.589	205.158	57.485	66.794	81.222	324.141	19.78
728.633	602.986	189.859	57.085	63.785	82.000	302.370	28.21
754.057	636.958	181.101	56.805	59.788	82.918	288.437	36.46
638.992	527.280	178.968	55.970	64.889	83.770	286.361	55.00
606.110	501.980	165.999	55.727	64.948	84.600	268.955	65.08
EGT #1	EGT #2	EGT #4	EGT #5	EGT #8	Air Temp.	Air Flow	
657.864	518.115	213.806	57.361	78.098	80	341.579	
652.766	513.389	213.650	57.050	78.564	80	339.470	
656.403	516.933	213.619	57.330	78.440	80	341.630	
658.642	518.581	213.806	57.299	78.658	80	346.532	
655.533	515.223	213.744	57.112	79.590	80	346.929	
658.175	517.369	213.992	57.206	78.254	80	344.790	
656.154	515.192	214.024	57.050	79.280	80	345.566	
660.196	518.643	214.272	57.237	78.875	80	348.963	
661.626	519.452	214.614	57.237	78.627	80	348.739	
660.849	518.674	214.832	57.206	78.347	80	346.015	
660.072	517.742	214.770	57.175	78.689	80	345.342	
660.942	518.364	214.956	57.112	78.627	80	348.171	
663.989	520.726	215.392	57.361	78.409	80	348.912	
661.688	518.301	215.298	57.112	77.849	80	346.757	
661.222	517.959	215.423	57.081	79.217	80	344.963	
661.813	518.643	215.485	57.112	78.844	80	347.550	
664.642	521.037	215.765	57.206	78.378	80	349.480	
667.254	523.493	216.044	57.392	77.010	80	347.774	
666.103	522.467	215.982	57.361	78.005	80	345.739	
663.181	519.576	215.920	57.206	78.627	80	348.119	
669.212	524.924	216.511	57.423	77.818	80	350.342	
666.725	522.467	216.449	57.361	77.570	80	348.050	
667.222	523.120	216.635	57.361	77.476	80	345.118	
668.155	523.867	216.791	57.423	77.849	80	347.205	
664.642	520.167	216.635	57.206	78.938	80	350.066	
669.492	524.582	216.946	57.361	77.196	80	348.791	
659.481	514.975	216.386	56.739	71.818	80	345.566	
663.119	518.332	216.853	57.050	74.834	80	347.153	
669.865	524.924	217.133	57.454	77.849	80	349.894	
666.539	521.410	217.412	57.330	80.741	80	348.963	
671.202	526.074	217.630	57.485	79.435	80	345.635	
665.544	520.758	217.195	57.361	79.808	80	345.187	
668.497	523.462	217.475	57.548	79.217	80	347.895	

Table 3: Optrand pressure averaging spreadsheet sample.

Pressure Curve Avg., 2100 RPM, 50% Load, 0% H2,									
Time per sample		RPM	Deg/s	Deg/sampling Period		SCFM H2	% H2 Energy		
6.94444E-05		2100	12600	0.8750		0	0		
Time	Deg	1	2	3	4	5	6	7	AVG
0.0000	296.3	0.598	0.602	0.601	0.605	0.600	0.599	0.604	0.601
0.0001	297.1	0.605	0.603	0.603	0.605	0.594	0.599	0.607	0.603
0.0001	298.0	0.610	0.608	0.600	0.608	0.611	0.614	0.610	0.608
0.0002	298.9	0.610	0.613	0.602	0.614	0.608	0.610	0.611	0.612
0.0003	299.8	0.617	0.618	0.610	0.615	0.616	0.616	0.616	0.616
0.0003	300.6	0.619	0.621	0.614	0.620	0.622	0.620	0.619	0.621
0.0004	301.5	0.629	0.624	0.614	0.626	0.621	0.624	0.626	0.626
0.0005	302.4	0.630	0.631	0.620	0.627	0.634	0.627	0.632	0.631
0.0006	303.3	0.632	0.639	0.624	0.638	0.630	0.637	0.641	0.636
0.0006	304.1	0.637	0.642	0.632	0.638	0.637	0.640	0.644	0.641
0.0007	305.0	0.645	0.651	0.637	0.646	0.647	0.649	0.646	0.648
0.0008	305.9	0.655	0.656	0.641	0.655	0.651	0.655	0.661	0.655
0.0008	306.8	0.663	0.659	0.651	0.656	0.659	0.656	0.663	0.661
0.0009	307.6	0.663	0.670	0.661	0.662	0.662	0.659	0.673	0.667
0.0010	308.5	0.673	0.671	0.667	0.674	0.672	0.677	0.678	0.675
0.0010	309.4	0.680	0.684	0.672	0.684	0.676	0.678	0.681	0.682
0.0011	310.3	0.695	0.686	0.683	0.686	0.679	0.688	0.694	0.689
0.0012	311.1	0.700	0.697	0.686	0.692	0.696	0.696	0.707	0.698
0.0013	312.0	0.705	0.705	0.694	0.699	0.699	0.705	0.707	0.705
0.0013	312.9	0.712	0.717	0.703	0.713	0.713	0.713	0.713	0.715
0.0014	313.8	0.728	0.726	0.711	0.719	0.719	0.726	0.733	0.726
0.0015	314.6	0.735	0.734	0.716	0.732	0.728	0.733	0.738	0.734
0.0015	315.5	0.744	0.751	0.727	0.742	0.737	0.743	0.750	0.745
0.0016	316.4	0.755	0.764	0.739	0.757	0.745	0.751	0.758	0.757
0.0017	317.3	0.767	0.767	0.748	0.767	0.761	0.767	0.767	0.768
0.0017	318.1	0.777	0.780	0.754	0.773	0.777	0.774	0.783	0.779
0.0018	319.0	0.792	0.797	0.774	0.788	0.783	0.783	0.795	0.791
0.0019	319.9	0.810	0.808	0.780	0.804	0.791	0.801	0.808	0.805
0.0019	320.8	0.816	0.822	0.796	0.817	0.807	0.813	0.825	0.818
0.0020	321.6	0.832	0.831	0.808	0.834	0.823	0.823	0.835	0.833
0.0021	322.5	0.851	0.843	0.816	0.842	0.838	0.843	0.853	0.848
0.0022	323.4	0.860	0.876	0.842	0.858	0.850	0.855	0.865	0.865
0.0022	324.3	0.878	0.885	0.853	0.881	0.874	0.873	0.881	0.882
0.0023	325.1	0.899	0.904	0.867	0.897	0.882	0.894	0.904	0.899

Table 4: Oscilloscope data spreadsheet sample.

Comb. and Inj. Timing, 2100 RPM, 50% Load, 0% H2				
RPM	Deg/s	Deg/sampling Period	SCFM H2	% H2 Energy
2100	12600	1.2600	0	0
Memory Length		500		
Trigger Level		4.00E-01		
Source		CH1		
Vertical Units		V		
Vertical Scale		5.00E+00		
Vertical Position		0.00E+00		
Horizontal Units		s		
Horizontal Scale		2.50E-03		
Horizontal Position		-9.00E-04		
Horizontal Mode		Main		
Sampling Period		1.00E-04		
Firmwave		V1.04		
Time		6/22/2011 5:01		
Waveform Data				
Time	Deg	VR	INJ	Pressure
0	41.2200	2	1	15
0.0001	42.4800	3	1	16
0.0002	43.7400	2	1	15
0.0003	45.0000	3	1	16
0.0004	46.2600	2	1	15
0.0005	47.5200	2	1	15
0.0006	48.7800	2	1	16
0.0007	50.0400	1	1	16
0.0008	51.3000	3	1	16
0.0009	52.5600	3	1	16
0.001	53.8200	4	1	16
0.0011	55.0800	3	1	15
0.0012	56.3400	2	1	15
0.0013	57.6000	3	1	16
0.0014	58.8600	4	1	15
0.0015	60.1200	7	1	16
0.0016	61.3800	9	1	15
0.0017	62.6400	8	2	15
0.0018	63.9000	4	0	16
0.0019	65.1600	-2	2	15

Table 5: Exhaust emissions data spreadsheet sample.

2100 RPM 50% Load							
H2 Flow	% H2	% O2	%CO	%CO2	HC	NO	NO2
SCFM	Energy	%	%	%	PPM	PPM	PPM
0	0.00	13.2	0.02	6.4	1	77	198
3.7	10.49	13.5	0.01	6	1	83	440
7.3	19.78	13	0.01	5.9	1	115	520
11	28.21	12.7	0.03	6	1	139	517
14.3	36.46	12.1	0.03	5.8	1	255	494
18.3	55.00	13.3	0.01	4.2	1	367	44
20.8	65.08	13.1	0.01	3.8	1	433	399

APPENDIX B. THERMAL EFFICIENCY

The engine's thermal efficiency was analyzed for all test speeds. The thermal efficiency for the test speeds are presented in Figure 30. The thermal efficiency is another way of analyzing the same data as the SEC. It is included to provide reference to other engine's thermal efficiency.

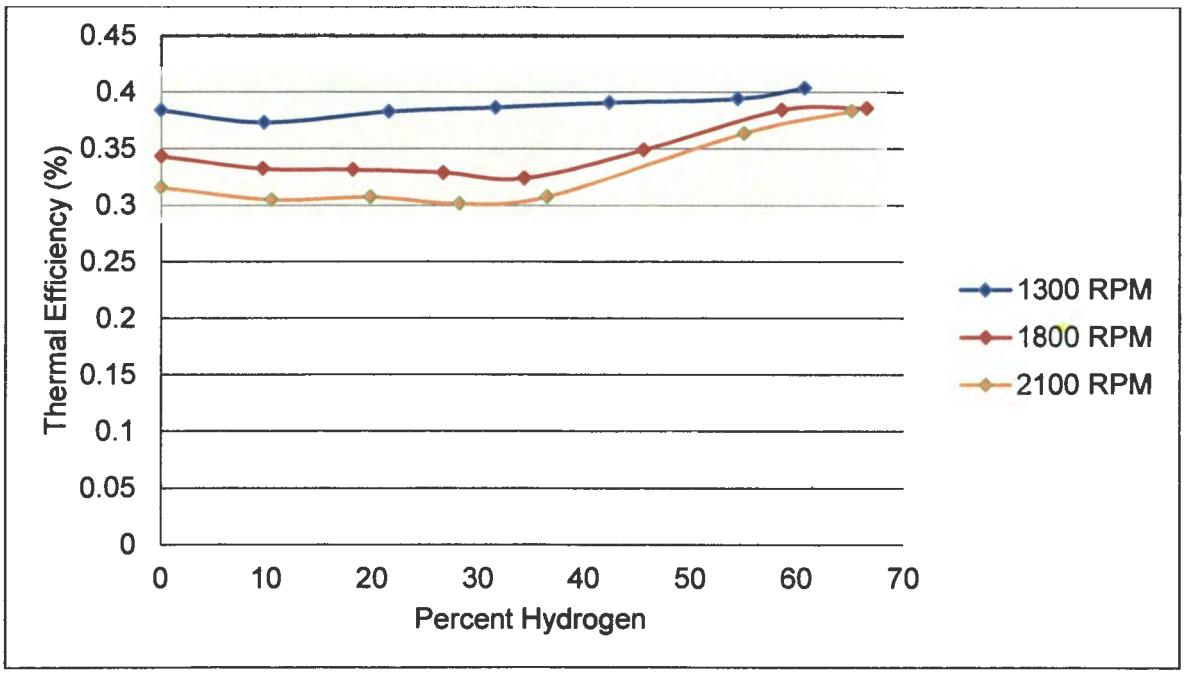

Figure 30: Thermal efficiencies for test speeds and various amounts of hydrogen.